

**Chiral non-Abelian vortices and their confinement in three flavor dense QCD**Minoru Eto<sup>1,2,\*</sup> and Muneto Nitta<sup>2,3,†</sup><sup>1</sup>*Department of Physics, Yamagata University,**Kojirakawa-machi 1-4-12, Yamagata, Yamagata 990-8560, Japan*<sup>2</sup>*Research and Education Center for Natural Sciences, Keio University,**4-1-1 Hiyoshi, Yokohama, Kanagawa 223-8521, Japan*<sup>3</sup>*Department of Physics, Keio University, 4-1-1 Hiyoshi, Kanagawa 223-8521, Japan*

(Received 10 August 2021; accepted 19 October 2021; published 30 November 2021)

We find chiral non-Abelian vortices having windings only in one of the diquark condensations of left-handed and right-handed quarks in the color-flavor locked phase of dense QCD. They are the minimum vortices carrying half color magnetic fluxes of those of non-Abelian semisuperfluid vortices (color magnetic flux tubes) and  $1/6$  quantized superfluid circulations of Abelian superfluid vortices. These vortices carry  $CP^2$  orientational moduli in the internal space corresponding to their fluxes. The  $CP^2$  moduli of two chiral non-Abelian vortices with chiralities opposite to each other are energetically favored to be aligned while those of a vortex and antivortex to be orthogonal, and then these vortices attract each other. They are attached by chiral domain walls in the presence of the mass and axial anomaly terms explicitly breaking axial and chiral symmetries. We numerically show that two chiral non-Abelian vortices with chiralities opposite to each other are connected by a chiral domain wall, consisting a mesonic bound state which is nothing but a non-Abelian semisuperfluid vortex. We also show that Abelian and non-Abelian axial vortices attached by chiral domain walls are all unstable to decay into a set of chiral non-Abelian vortices. Furthermore, we find that chiral non-Abelian vortices exhibit unique features: One is the so-called topological obstruction implying that unbroken symmetry generators in the bulk are not defined globally around the vortices, and the other is color nonsinglet Aharonov-Bohm (AB) phases implying that quarks encircling these vortices can detect the colors of magnetic fluxes of them at infinite distances.

DOI: [10.1103/PhysRevD.104.094052](https://doi.org/10.1103/PhysRevD.104.094052)**I. INTRODUCTION**

What states of matter are at extreme conditions is one of the challenging problems in modern physics. The ground state of the cold QCD matter at high densities is expected to exhibit color superconductivity, which may be realized in cores of neutron stars [1]. Various phases have been proposed for color superconductivity; the color-flavor locked (CFL) phase [2] in three-flavor symmetric matter is realized extremely high density limit, while the two-flavor superconducting (2SC) phase [3,4] was also proposed for two-flavor symmetric matter. If a color superconductor is realized in the core of neutron stars, there must appear quantum vortices, i.e., vortices with quantized circulations, because of rapid rotations. In color-superconducting quark matter,

quantum vortices or color magnetic flux tubes appear, as reviewed in Ref. [5]. In the CFL phase, Abelian superfluid vortices are created by rotations [6,7], which are dynamically unstable to decay into more stable vortices [8–10]. The most stable vortices are non-Abelian semisuperfluid vortices carrying color magnetic fluxes and  $1/3$  circulation of the Abelian superfluid vortices [5,8,11–13], which are analogous to non-Abelian vortices in supersymmetric QCD [14–19] (see Refs. [20–23] as a review) and two-Higgs doublet models [24–28]. A non-Abelian vortex confines massless particles in its core; one type is bosonic Nambu-Goldstone  $CP^2$  modes originated from spontaneous breaking of the CFL symmetry in its core [5,8,29,30], and the other is gapless Majorana fermions with more a topological origin [31–33]. Under a rapid rotation, there appear a huge number of vortices (about  $10^{19}$  for typical neutron stars). They will form a vortex lattice [34] that behaves as a polarizer of photons [35]. One of the most recent pieces of progress is vortices penetrating through crossover between the CFL phase and hyperon nuclear matter within a quark-hadron continuity [9,36–42]. While it was suggested that one superfluid vortex in the hyperon nuclear matter is connected to one non-Abelian vortex in the CFL phase [36], it was

\*meto@sci.kj.yamagata-u.ac.jp

†nitta@phys-h.keio.ac.jp

Published by the American Physical Society under the terms of the [Creative Commons Attribution 4.0 International license](https://creativecommons.org/licenses/by/4.0/). Further distribution of this work must maintain attribution to the author(s) and the published article's title, journal citation, and DOI. Funded by SCOAP<sup>3</sup>.

proved in Refs. [37,38] that three superfluid vortices meet three non-Abelian vortices at a point called a Boojum [9].

The CFL phase is characterized by the two diquark condensations of left and right-handed quarks  $q_{L,R}$ ,  $(\Phi_{L,R})_{aa} \sim \epsilon_{\alpha\beta\gamma}\epsilon_{abc}q_{L,R}^{\beta b}q_{L,R}^{\gamma c}$  with the color indices  $\alpha, \beta, \gamma = r, g, b$  and the flavor indices  $a, b, c = u, d, s$ . In the ground states, they both develop VEVs as  $\Phi_L = -\Phi_R$ . Thus, with defining  $\Phi \equiv \Phi_L = -\Phi_R$ , one has discussed non-Abelian vortices in terms of  $\Phi$  and gauge fields. However, since the relation  $\Phi_L = -\Phi_R$  holds only in the ground state, we do not have to assume it for excited states such as vortices. In fact, a similar situation can be found in two-component condensed matter systems: two-gap superconductors [43–46] and two-component Bose-Einstein condensates (BECs) [47–53]. In these systems, there are two condensations  $\Phi_1$  and  $\Phi_2$ . For a singly quantized vortex both fields have the winding  $\Phi_1 = \Phi_2 \sim e^{i\varphi}$  with azimuthal angle  $\varphi$ . However, they also admit so-called half-quantum vortices  $(\Phi_1, \Phi_2) \sim (e^{i\varphi}, 1)$  or  $(\Phi_1, \Phi_2) \sim (1, e^{i\varphi})$ , denoted as  $(1, 0)$  or  $(0, 1)$ , respectively. It is called half-quantum since it carries a half magnetic flux in superconductors or half circulation in BECs.<sup>1</sup> When the system contains an interaction term  $\Phi_1^*\Phi_2 + \text{c.c.}$  known as a Josephson term in superconductors or Rabi coupling in BECs,  $(1, 0)$  and  $(0, 1)$  vortices are connected by a sine-Gordon soliton [44,45,47]<sup>2</sup>; they are confined to form a singly quantized vortex. When there are no such terms, they are deconfined and are weakly interacting each other. Thus, one may wonder if the same can be considered for vortices in the CFL phase.

In this paper, we investigate non-Abelian vortices having windings only in left  $\Phi_L$  or right  $\Phi_R$  condensation, while the previously known non-Abelian vortices have windings in the both components simultaneously. We call them ‘‘chiral non-Abelian vortices’’ in the sense that quarks of only left or right chirality participate in the vortices. A single non-Abelian semisuperfluid vortex can be decomposed into chiral non-Abelian vortices of chiralities opposite to each other. Chiral non-Abelian vortices carry half color magnetic fluxes of those of non-Abelian semisuperfluid vortices and  $1/6$  quantized superfluid circulations of Abelian superfluid vortices. We find that a single chiral non-Abelian vortex carries  $\mathbb{C}P^2$  orientational moduli in the internal space corresponding to its color magnetic flux. As the case of the Josephson or Rabi term for two-component condensed matter systems, a chiral non-Abelian vortex is attached by a

chiral domain wall [5,54] in the presence of mass and axial anomaly terms explicitly breaking axial and chiral symmetries. We also study energetics of two chiral vortices in the absence of mass and axial anomaly terms. In the coexistence of a set of two chiral vortices with opposite chiralities, their  $\mathbb{C}P^2$  moduli must be aligned energetically and they attract each other. On the other hand, in the coexistence of a chiral vortex and an antichiral vortex, their  $\mathbb{C}P^2$  moduli are energetically orthogonal to each other, and they attract each other. We show that in the presence of mass or axial anomaly term, chiral non-Abelian vortices of opposite chirality are connected by a chiral domain wall and are linearly confined.

Other interesting features that we find in this paper are so-called *topological obstruction* (see the Appendix A 4) [55–62] and non-Abelian Aharonov-Bohm (AB) phases. First, the topological obstruction that chiral non-Abelian vortices exhibit implies that generators of the unbroken symmetry in the ground state are not globally defined around the vortices. Second, the chiral non-Abelian vortices exhibit color nonsinglet (generalized) AB phases so that the quarks can detect the colors of magnetic fluxes of these vortices at large distances. The bound state of two chiral non-Abelian vortices with the opposite chiralities, equivalent to a single non-Abelian semisuperfluid vortex at large distance, exhibits only color singlet (generalized) AB phases so that the quarks cannot detect the color magnetic flux of such a bound state at large distances.

Finally, we will point out that chiral non-Abelian vortices are the most fundamental elements among topological solitons formed during the chiral symmetry breaking. The CFL phase is accompanied by spontaneous breaking of the chiral symmetry since the diquark condensations  $\Phi_{L,R}$  of left and right-handed quarks  $q_{L,R}$  both develop VEVs. This breaking admits several vortices without color magnetic fluxes. When the  $U(1)_A$  axial symmetry is spontaneously broken, it admits an axial vortex winding around  $U(1)_A$ . This vortex is attached by  $2N$  domain walls because of the anomaly term explicitly breaking the  $U(1)_A$  axial symmetry, in contrast to an analogous axial string in the linear sigma model for chiral symmetry breaking which is attached by  $N$  domain walls [63]. The  $U(N)_L \times U(N)_R$  chiral symmetry breaking admits a non-Abelian axial string, which is attached by one (or two) chiral domain wall(s) depending on the form of mass terms, analogous to one in the linear sigma model for chiral symmetry breaking [12,64–67]. The  $U(1)_A$  Abelian axial vortex mentioned above is dynamically split into  $N$  non-Abelian axial strings by domain wall tensions, where each non-Abelian string is attached by one (or two) chiral domain wall(s), as an analogous decay was studied in the linear sigma model for chiral symmetry breaking [5,54]. We find that a single non-Abelian axial string decays into a pair of a chiral non-Abelian vortex and an antichiral non-Abelian vortex, while a single Abelian axial string decays into a set of  $N$  chiral non-Abelian vortices and  $N$  antichiral non-Abelian

<sup>1</sup>Strictly speaking, they are half quantized when the VEVs of  $\Phi_1$  and  $\Phi_2$  are the same. When their VEVs  $\langle \Phi_1 \rangle = v_1$ ,  $\langle \Phi_2 \rangle = v_2$  are different, they are fractionally quantized as  $v_1^2/(v_1^2 + v_2^2)$  and  $v_2^2/(v_1^2 + v_2^2)$ .

<sup>2</sup>While the Josephson coupling is inevitable in superconductors, the Rabi coupling is in general absent in BECs and one can introduce it as an experimentally controllable parameter.

vortices. Thus, chiral non-Abelian vortices are the most fundamental strings.<sup>3</sup>

This paper is organized as follows. In Sec. II, we review the Ginzburg-Landau (GL) theory paying attention to symmetries, and give the order parameter manifold (OPM) which is a new result. In Sec. III, we review superfluid vortices: Abelian  $U(1)_B$  superfluid vortices and non-Abelian semi-superfluid vortices (color flux tubes). In Sec. IV, we discuss Abelian and non-Abelian axial vortices. In Sec. V, we construct chiral non-Abelian vortices in the absence of chiral symmetry breaking terms, and show that they exhibit the topological obstruction and (generalized) AB phases of quarks encircling them. In Sec. VI, we discuss energetics of a single chiral non-Abelian vortex, non-Abelian semi-superfluid vortex, non-Abelian axial vortex, and more general composite vortices. We find that the  $CP^2$  orientations of two chiral vortices with the opposite chiralities are energetically favored to be aligned to each other and then they attract each other, while those of chiral vortex and antivortex with the opposite chiralities are energetically favored to be orthogonal to each other and then they attract each other. In Sec. VII, we show that Abelian and non-Abelian axial vortices are attached by chiral domain walls in the presence of axial and chiral symmetry breaking terms, and discuss decay of these vortices. In Sec. VIII, we construct a mesonic bound state of two chiral non-Abelian vortices with the opposite chiralities. Section IX is devoted to a summary and discussion. In Appendix A, the terminologies used in this paper are summarized. In Appendix B, we give detailed discussions on symmetry breakings in the CFL phase, and determine associated OPMs. In Appendix C, chiral non-Abelian vortices in the CFL phase are compared with non-Abelian Alice strings [68–70] in the 2SC +  $dd$  phase of two-flavor quark matter proposed recently [71,72].

## II. COLOR-FLAVOR LOCKED PHASE OF THREE FLAVOR QUARK MATTER

In this section, after we review the color-flavor locked phase of dense QCD, we give OPMs and their topology as a new result.

The (approximate) symmetry of  $N$  flavor quark matter is (up to discrete groups)

$$G = SU(N)_C \times U(1)_B \times U(1)_A \times SU(N)_L \times SU(N)_R, \quad (2.1)$$

<sup>3</sup>The chiral non-Abelian vortex can be considered as a hybrid of a non-Abelian semisuperfluid vortex (color flux tube) and a non-Abelian axial string: the former winds around  $\Phi_L$  and  $\Phi_R$  with the same windings, the latter winds around them with the opposite windings, and the chiral non-Abelian vortex winds around only either of  $\Phi_L$  and  $\Phi_R$ , achieved by a half non-Abelian semisuperfluid vortex (color flux tube) and a half non-Abelian axial string.

where  $SU(N)_C$  is the color gauge group, and the rests are global symmetries:  $U(1)_B$ ,  $U(1)_A$ , and  $SU(N)_L \times SU(N)_R$  are baryon number, axial, and chiral symmetries, respectively. See Appendix B for a more precise description including discrete groups. The light quarks  $q_{L,R} = (q_{L,R})_{\alpha a}$  with  $\alpha = 1, 2, \dots, N$  ( $\alpha = r, g, b$  for  $N = 3$ ),  $a = 1, 2, \dots, N$  ( $a = u, d, s$  for  $N = 3$ ), and heavy quarks  $Q_{L,R} = (Q_{L,R})_\alpha$  transform under  $G$  as

$$\begin{aligned} q_L &\rightarrow e^{i\theta_B/2} e^{i\theta_A/2} g_C^* q_L U_L^T, & q_R &\rightarrow e^{i\theta_B/2} e^{-i\theta_A/2} g_C^* q_R U_R^T \\ Q_L &\rightarrow g_C^* Q_L, & Q_R &\rightarrow g_C^* Q_R, \end{aligned} \quad (2.2)$$

where we have not introduced heavy quark flavor symmetry, and have assigned no  $U(1)_B$  and  $U(1)_A$  charges on the heavy quarks.<sup>4</sup> The case of  $N = 3$  corresponds to the CFL phase of dense QCD, in which case the light quarks constitute diquark condensations as  $(\Phi_{L,R})_{\alpha a} \sim \epsilon_{\alpha\beta\gamma} \epsilon_{abc} q_{L,R}^{\beta b} q_{L,R}^{\gamma c}$ . Hereafter, we mostly consider the condensates  $(\Phi_{L,R})_{\alpha a}$  as  $N$  by  $N$  matrices of complex scalar fields on which the symmetries  $G$  act as

$$\begin{aligned} \Phi_L &\rightarrow e^{i\theta_B + i\theta_A} g_C \Phi_L U_L^\dagger, & \Phi_R &\rightarrow e^{i\theta_B - i\theta_A} g_C \Phi_R U_R^\dagger \\ g_C &\in SU(N)_C, & U_{L,R} &\in SU(N)_{L,R}, & e^{i\theta_B} &\in U(1)_B, \\ e^{i\theta_A} &\in U(1)_A. \end{aligned} \quad (2.3)$$

The vector symmetry  $SU(N)_{L+R}$  given by  $U_L = U_R$  is a subgroup of the chiral symmetry  $SU(N)_L \times SU(N)_R$ , and the rest of generators outside  $SU(N)_{L+R}$  defines the coset space  $[SU(N)_L \times SU(N)_R]/SU(N)_{L+R} \simeq SU(N)$  which we sometimes denote  $SU(N)_{L-R}$  although this does not form a group.

In this paper, we use the static GL free energy for studying vortices. The GL Lagrangian for the CFL phase was obtained as [73–75]

$$\mathcal{L} = \text{Tr} \left[ -\frac{1}{4} F^{ij} F_{ij} + \mathcal{D}_i \Phi_L^\dagger \mathcal{D}^i \Phi_L + \mathcal{D}_i \Phi_R^\dagger \mathcal{D}^i \Phi_R \right] - V, \quad (2.4)$$

<sup>4</sup>The antifundamental representation  $*$  of quarks for the color group is a convention to make the representation of the condensations  $\Phi_{L,R}$  introduced below to be fundamental in Eq. (2.3), below. The situation in our mind is that only the light quarks are condensed by forming diquark pairs while the heavy quarks are not. Thus, we use the terminology “ $U(1)_B$  baryon symmetry” for the spontaneously broken baryon symmetry associated only with the light quarks with no charges for the heavy quarks, while the heavy quarks are also charged under the conventional baryon symmetry.

$$\begin{aligned}
V = & -\frac{m^2}{2} \text{Tr}[\Phi_L^\dagger \Phi_L + \Phi_R^\dagger \Phi_R] + \frac{\lambda_1}{4} \text{Tr}[(\Phi_L^\dagger \Phi_L)^2 \\
& + (\Phi_R^\dagger \Phi_R)^2] + \frac{\lambda_2}{4} (\text{Tr}[\Phi_L^\dagger \Phi_L]^2 + \text{Tr}[\Phi_R^\dagger \Phi_R]^2) \\
& + \frac{\lambda_3}{2} \text{Tr}[\Phi_L^\dagger \Phi_L] \text{Tr}[\Phi_R^\dagger \Phi_R] + \frac{\lambda_4}{2} \text{Tr}[\Phi_L \Phi_L^\dagger \Phi_R \Phi_R^\dagger] \\
& + [\gamma_1 \text{Tr}(\Phi_L^\dagger \Phi_R) + \gamma_2 \text{Tr}[(\Phi_L^\dagger \Phi_R)^2] \\
& + \gamma_3 \det(\Phi_L^\dagger \Phi_R) + (\text{c.c.})], \tag{2.5}
\end{aligned}$$

where the GL coefficients depending on the temperature, density, and so on can be found in Refs. [73–75]. Among the global symmetries, the axial  $U(1)_A$  and chiral symmetries are explicitly broken in the presence of the last terms for  $\gamma_{1,2,3} \neq 0$  with  $U(1)_B \times SU(N)_{L+R}$  remaining exact. The GL theory is valid only near the transition temperature  $T_c$ . Beyond the GL theory, we need Bogoliubov–de Gennes (BdG) formulation [31,32].

The ground state is given by

$$\Phi_L = -\Phi_R = v \mathbf{1}_N, \quad v \equiv \left( \frac{m^2}{\lambda_1 + N\lambda_2 + N\lambda_3} \right)^{\frac{1}{4}} \tag{2.6}$$

for small  $\gamma$ 's. The symmetry  $G$  is spontaneously broken down to the CFL symmetry given by

$$H = SU(N)_{C+L+R}, \quad g_C = U_L = U_R. \tag{2.7}$$

The chiral symmetry,  $U(1)_A$  and  $U(1)_B$  symmetries are spontaneously broken.

According to Appendix B, the full OPM for the symmetry breaking can be written, with taking into account discrete groups, as

$$\begin{aligned}
\mathcal{M} = & \frac{G}{H} \simeq \frac{U(N)_{C-(L+R)+B} \times U(N)_{L-R+A}}{(\mathbb{Z}_2)_{A+B}} \\
= & \frac{\mathcal{M}_V \times \mathcal{M}_A}{(\mathbb{Z}_2)_{A+B}}, \tag{2.8}
\end{aligned}$$

where  $(\mathbb{Z}_2)_{A+B}$  is generated by  $(-1, -1) \in U(1)_B \times U(1)_A$ , and  $F \times B$  denotes a fiber bundle with a fiber  $F$  over a base manifold  $B$ . Here, we have defined the sub-OPMs for the vector symmetry breaking and for the axial and chiral symmetry breakings by

$$\begin{aligned}
\mathcal{M}_V \simeq & U(N)_{C-(L+R)+B} \simeq \frac{U(1)_B \times SU(N)_{C-(L+R)}}{(\mathbb{Z}_N)_{C-(L+R)+B}}, \\
\mathcal{M}_A \simeq & U(N)_{L-R+A} \simeq \frac{U(1)_A \times SU(N)_{L-R}}{(\mathbb{Z}_N)_{L-R+A}}, \tag{2.9}
\end{aligned}$$

respectively, with coset spaces

$$\begin{aligned}
SU(N)_{C-(L+R)} & \simeq \frac{SU(N)_C \times SU(N)_{L+R}}{SU(N)_{C+L+R}}, \\
SU(N)_{L-R} & \simeq \frac{SU(N)_L \times SU(N)_R}{SU(N)_{L+R}}. \tag{2.10}
\end{aligned}$$

For the details of derivation, see Appendix B.

The  $(\mathbb{Z}_2)_{A+B}$  in the denominator of Eq. (2.8) was not recognized before (see Eq. (2.26) of Ref. [5]), and this is a key point to understand chiral non-Abelian vortices found in this paper. The nontrivial first homotopy groups of the sub-OPMs

$$\pi_1(\mathcal{M}_V) \simeq \mathbb{Z}, \quad \pi_1(\mathcal{M}_A) \simeq \mathbb{Z} \tag{2.11}$$

support non-Abelian semisuperfluid vortices (Sec. III B) and non-Abelian axial vortices (Sec. IV B), respectively, but they are not the minimum vortices. On the contrary, the nontrivial first homotopy group of the full OPM

$$\pi_1(\mathcal{M}) \simeq \mathbb{Z} \tag{2.12}$$

supports chiral non-Abelian vortices as the minimum vortices.

Here, one comment is in order. Considering  $N = 1$  in the full OPM in Eq. (2.8), we obtain the OPM for two-component BECs or superconductors, see Ref. [76], allowing half-quantized vortices. Thus, our case is a non-Abelian generalization of such two-component condensed matter systems.

For later conveniences, we define gauge invariants

$$\Sigma \equiv \Phi_R^\dagger \Phi_L \quad \det \Phi_L, \quad \det \Phi_R. \tag{2.13}$$

Here,  $\Sigma$  is the chiral symmetry breaking order parameter. These gauge invariants transform under the flavor symmetry as

$$\begin{aligned}
\Sigma & \rightarrow e^{2i\theta_A} U_R \Sigma U_L^\dagger \\
\det \Phi_L & \rightarrow e^{Ni\theta_B + Ni\theta_A} \det \Phi_L, \\
\det \Phi_R & \rightarrow e^{Ni\theta_B - Ni\theta_A} \det \Phi_R. \tag{2.14}
\end{aligned}$$

In the following sections, we classify various vortices in the CFL phase as summarized in Table I. To this end, let us introduce labels of vortices by

$$(m, n): \det \Phi_L \sim e^{im\varphi}, \quad \det \Phi_R \sim e^{in\varphi}, \tag{2.15}$$

with winding numbers  $n$  and  $m$  of the gauge invariants  $\det \Phi_L$  and  $\det \Phi_R$ , respectively. Here  $\varphi$  is the angle coordinate of the polar coordinates in two dimensional space perpendicular to the vortex.

TABLE I. A summary table for various vortices and color magnetic flux tubes. The  $N = 3$  case corresponds to those in the CFL phase of dense QCD. NA denotes “non-Abelian.” “OPM” implies the sub-OPM that vortices are supported by nontrivial first homotopy groups  $\pi_1$  (OPM), except for color flux tubes which are topologically trivial:  $\pi_1(SU(N)_C) = 0$ .  $\mathcal{M}_V$ ,  $\mathcal{M}_A$ , and  $\mathcal{M}$  are the OPM for vector symmetry breaking, OPM for axial and chiral symmetry breakings, and full OPM defined in Eqs. (2.9) and (2.8). See Appendix B for details of these OPMs. “Chiral circulation” would imply an amount of magnetic fluxes if the chiral symmetry is gauged, where the normalization is taken such that a closed loop in  $SU(N)_{L-R}$  gives a unit flux.

Vortex	OPM	Label	$U(1)_B$ circulation	Color magnetic flux	$U(1)_A$ winding	Chiral circulation
Pure color magnetic flux tube	$SU(N)_C$	(0, 0)	0	1	0	0
Abelian superfluid vortex	$U(1)_B$	( $N, N$ )	1	0	0	0
NA semisuperfluid vortex	$\mathcal{M}_V$	(1, 1)	$\frac{1}{N}$	$\frac{1}{N}$	0	0
Abelian axial vortex	$U(1)_A$	( $N, -N$ )	0	0	1	0
NA axial vortex	$\mathcal{M}_A$	(1, -1)	0	0	$\frac{1}{N}$	$\frac{1}{N}$
Chiral NA vortex	$\mathcal{M}$	(1, 0) or (0, 1)	$\frac{1}{2N}$	$\frac{1}{2N}$	$\frac{1}{2N}$	$\frac{1}{2N}$

### III. SUPERFLUID VORTICES AND COLOR MAGNETIC FLUX TUBES

In this section, we review superfluid vortices in the CFL phase: Abelian superfluid vortices and non-Abelian semisuperfluid vortices.

#### A. Abelian superfluid vortices

The simplest vortex is an Abelian superfluid vortex winding around  $U(1)_B$  [6,7], given in the polar coordinates  $(r, \varphi)$  by

$$\Phi_L = -\Phi_R = e^{i\varphi} f(r) \mathbf{1}_N = e^{i\theta_B(\varphi)} f(r) \mathbf{1}_N, \quad (3.1)$$

with  $e^{i\theta_B(\varphi)} = e^{i\varphi}$  and the profile function  $f$  with the boundary conditions  $f(r=0) = 0$  and  $f(r=\infty) = v$ . This is unstable to decay into  $N$  non-Abelian semisuperfluid vortices introduced in Sec. III B [8–10].

In this notation of Eq. (2.15), the Abelian superfluid vortex is labeled by  $(N, N)$  because of  $\det \Phi_L \sim \det \Phi_R \sim e^{Ni\varphi}$ . The gauge invariant  $\Sigma$  is  $\Sigma = f^2 \mathbf{1}_N$  having no winding.

#### B. Non-Abelian semisuperfluid vortices

In this subsection, we review non-Abelian semisuperfluid vortices (color magnetic flux tubes) for comparison with chiral non-Abelian vortices introduced in Sec. V. The ansatz for a single non-Abelian semisuperfluid vortex winding around the sub-OPM  $\mathcal{M}_V \simeq U(N)_{C-(L+R)+B}$  for the vector symmetry breaking is given in the polar coordinates  $(r, \varphi)$  by

$$\begin{aligned} \Phi_L = -\Phi_R &= \begin{pmatrix} f(r)e^{i\varphi} & 0 \\ 0 & g(r)\mathbf{1}_{N-1} \end{pmatrix} \\ &= e^{i\frac{\varphi}{N}} e^{i\frac{\varphi}{N} T_N} \begin{pmatrix} f(r) & 0 \\ 0 & g(r)\mathbf{1}_{N-1} \end{pmatrix} \\ &= e^{i\theta_B(\varphi)} U(\varphi) \begin{pmatrix} f(r) & 0 \\ 0 & g(r)\mathbf{1}_{N-1} \end{pmatrix}, \\ A_i &= -\epsilon_{ij} \frac{x^j}{Ng_s r^2} (1 - h(r)) T_N \end{aligned} \quad (3.2)$$

with

$$T_N = \text{diag.}(N-1, -1, \dots, -1) \quad (3.3)$$

and

$$e^{i\theta_B(\varphi)} = e^{i\varphi/N}, \quad U(\varphi) = e^{i\frac{\varphi}{N} T_N}, \quad (3.4)$$

with the boundary condition for the profile functions  $f$ ,  $g$  and  $h$

$$(f, g, h)_{r=0} = (0, 0, 1), \quad (f, g, h)_{r=\infty} = (v, v, 0). \quad (3.5)$$

Explicit numerical solutions were constructed in Ref. [13]. This carries a  $1/N$   $U(1)_B$  circulation compared with a unit circulation of an Abelian superfluid vortex given in Eq. (3.1), and a color magnetic flux which is  $1/N$  of that of a pure color flux tube generated by a closed loop in the  $SU(N)_C$  gauge group [77]. The latter is unstable to decay into the ground state due to the trivial first homotopy group  $\pi_1[SU(N)_C] = 0$ . In terms of the gauge invariants, the non-Abelian semisuperfluid vortex is labeled by (1, 1) because of  $\det \Phi_L \sim \det \Phi_R \sim e^{i\varphi}$ .

More generally, the  $SU(N)_{C+L+R}$  transformation on the ansatz in Eq. (3.2) yields a continuous family of solutions. They are characterized by the moduli space [5,8,12]

$$\mathbb{C}P^{N-1} = \frac{SU(N)_{C+L+R}}{SU(N-1) \times U(1)}. \quad (3.6)$$

These modes are normalizable [5,30], and their effective world-sheet Lagrangian was constructed in a singular gauge [5,30] and a regular gauge [78]. The gauge invariant  $\Sigma$  is  $\Sigma = \text{diag}(f^2, g^2, \dots, g^2)$  having no winding. This can represent the  $\mathbb{C}P^{N-1}$  orientation in Eq. (3.6) at  $r=0$ :  $\Sigma(r=0) = \text{diag}(0, *, \dots, *)$  with  $*$  being a nonzero constant in the case of the orientation in Eq. (3.2). Or, we may define the orientational vector  $\phi \in \mathbb{C}^N$  by  $\phi \cdot \Sigma = 0$ , giving rise to  $\phi^T = (*, 0, \dots, 0)$  in the case of the orientation in Eq. (3.2) [19,21].

The Abelian superfluid vortex is dynamically unstable to decay into  $N$  non-Abelian semisuperfluid vortices [8–10]. This decay process can be expressed as

$$(N, N) \rightarrow N(1, 1). \quad (3.7)$$

#### IV. ABELIAN AND NON-ABELIAN AXIAL VORTICES

In this section, we discuss Abelian and non-Abelian axial vortices, which are global vortices without any color fluxes.

##### A. Abelian axial vortices

First, let us turn off the axial and chiral symmetry breaking terms by  $\gamma_1 = \gamma_2 = \gamma_3 = 0$ . A single Abelian axial vortex winding around  $U(1)_A$  is given by

$$\Phi_L = -\Phi_R^\dagger = e^{i\varphi} f(r) \mathbf{1}_N = e^{i\theta_A(\varphi)} f(r) \mathbf{1}_N, \quad (4.1)$$

with  $e^{i\theta_A(\varphi)} = e^{i\varphi}$  and the profile function  $f$  with the boundary conditions  $f(r=0) = 0$  and  $f(r=\infty) = v$ . This vortex is labeled by  $(N, -N)$  because of  $\det \Phi_L \sim e^{Ni\varphi}$  and  $\det \Phi_R \sim e^{-Ni\varphi}$ .

In the presence of the axial and chiral symmetry breaking terms,  $\gamma_{1,2,3} \neq 0$ , domain walls are attached to the vortex. To see this, we consider an infinitely large circle with the spatial angle  $\varphi$  encircling the axial vortex. Then, let us substitute the ansatz in Eq. (4.1) to the potential  $V$  in Eq. (2.5), with replacing the spatial angle  $\varphi$  by a function  $\phi(\varphi)$  depending on the angle  $\varphi$  with the boundary condition  $\phi(\varphi=0) = 0$  and  $\phi(\varphi=2\pi) = 2\pi$ . Then, the potential can be evaluated at spatial infinities as

$$V = 2N\gamma_1 \cos(2\phi(\varphi)) + 2N\gamma_2 \cos(4\phi(\varphi)) + 2\gamma_3 \cos(2N\phi(\varphi)). \quad (4.2)$$

Along the large circle at infinity encircling the axial vortex, there is also the gradient term. Thus, the effective energy for

$\phi$  at the large circle becomes  $\mathcal{E}_{\text{eff}} = Nv^2(\partial_\varphi \phi)^2 + V$ . This is a variant of an  $N$ -ple sine-Gordon model.

In the case of  $(\gamma_1, \gamma_2, \gamma_3) = (0, 0, \gamma_3)$ , the Abelian axial vortex is attached by  $2N$  domain walls. In this case, this vortex is unstable to decay into  $N$  non-Abelian axial vortices introduced in Sec. IV B, each of which is attached by two domain walls. See discussion in Sec. VII B.

If we turn on  $\gamma_{1,2}$ , these  $2N$  domain walls would constitute a composite wall in general. It is an open question whether the decay is suppressed or not in such a case.

Before closing this subsection, let us mention a relation to analogous axial vortices in the context of chiral symmetry breaking at low density. In that case, the axial vortex is attached by  $N$  domain walls [63], and it decays into non-Abelian global strings each of which is attached by one domain wall [5,54]. To compare these two cases, it is convenient to see the gauge invariant  $\Sigma$  in Eq. (2.13). In terms of this gauge invariant, the axial vortex in Eq. (4.1) can be rewritten as

$$\Sigma = -e^{2i\varphi} f^2(r) \mathbf{1}_N = -e^{2i\theta_A(\varphi)} f^2(r) \mathbf{1}_N. \quad (4.3)$$

Thus, one can see that the minimum winding of the axial vortex in the CFL phase corresponds to the double winding of the axial vortex at low density [5,54,63].

##### B. Non-Abelian axial vortices

Here we discuss non-Abelian axial vortices winding in the sub-OPM  $\mathcal{M}_A = U(N)_{L-R+A}$  for the axial and chiral symmetry breakings. An analogue of this at low density was discussed in linear sigma models in Refs. [12,64–67]. First, let us turn off the axial and chiral symmetry breaking terms by  $\gamma_1 = \gamma_2 = \gamma_3 = 0$ .

The ansatz for a single non-Abelian axial vortex is given in the polar coordinates  $(r, \varphi)$  by

$$\begin{aligned} \Phi_L &= \begin{pmatrix} f(r)e^{i\varphi} & 0 \\ 0 & g(r)\mathbf{1}_{N-1} \end{pmatrix} \\ &= e^{\frac{i}{N}\varphi} \begin{pmatrix} f(r) & 0 \\ 0 & g(r)\mathbf{1}_{N-1} \end{pmatrix} e^{\frac{i}{N}\varphi T_N} \\ &= e^{i\theta_A(\varphi)} \begin{pmatrix} f(r) & 0 \\ 0 & g(r)\mathbf{1}_{N-1} \end{pmatrix} U(\varphi), \\ -\Phi_R &= \begin{pmatrix} f(r)e^{-i\varphi} & 0 \\ 0 & g(r)\mathbf{1}_{N-1} \end{pmatrix} \\ &= e^{-\frac{i}{N}\varphi} \begin{pmatrix} f(r) & 0 \\ 0 & g(r)\mathbf{1}_{N-1} \end{pmatrix} e^{-\frac{i}{N}\varphi T_N} \\ &= e^{-i\theta_A(\varphi)} \begin{pmatrix} f(r) & 0 \\ 0 & g(r)\mathbf{1}_{N-1} \end{pmatrix} U^\dagger(\varphi), \end{aligned} \quad (4.4)$$

with

$$e^{i\theta_A(\varphi)} = e^{i\varphi/N}, \quad U(\varphi) = e^{\frac{i}{N}\varphi T_N}. \quad (4.5)$$

The boundary condition is

$$(f, g', h)_{r=0} = (0, 0, 1), \quad (f, g, h)_{r=\infty} = (v, v, 0). \quad (4.6)$$

Explicit numerical solutions can be found in Refs. [65,67]. This vortex is a purely global vortex without any color magnetic flux, carrying a  $U(1)_A$  winding number which is  $1/N$  of that of the Abelian axial vortex in Eq. (4.1). The non-Abelian axial vortex is labeled by  $(1, -1)$  because of  $\det \Phi_L \sim e^{i\varphi}$  and  $\det \Phi_R \sim e^{-i\varphi}$ .

A set of solutions has  $\mathbb{C}P^{N-1}$  moduli, which are non-normalizable since the  $SU(N)_{L+R}$  transformation changes the boundary.

In the presence of the axial and chiral symmetry breaking terms,  $\gamma_{1,2,3} \neq 0$ , domain walls are attached to the vortex. In order to understand domain walls attached to the non-Abelian axial vortex, let us substitute the ansatz in Eq. (4.4) to the potential  $V$  in (2.5), with replacing the spatial angle  $\varphi$  by a function  $\phi(\varphi)$  depending on the angle  $\varphi$  with the boundary condition  $\phi(\varphi=0) = 0$  and  $\phi(\varphi=2\pi) = 2\pi$ . Then, the potential can be evaluated at spatial infinities as

$$V = 2(\gamma_1 + \gamma_3) \cos(2\phi(\varphi)) + 2\gamma_2 \cos(4\phi(\varphi)). \quad (4.7)$$

Together with the gradient term, the effective energy for  $\phi$  on the large circle at infinity encircling the non-Abelian axial vortex becomes  $\mathcal{E}_{\text{eff}} = v^2(\partial_\varphi \phi)^2 + V$ . This is the double sine-Gordon model with a half periodicity  $\pi$  instead of the usual case of  $2\pi$ .

In the case of  $(\gamma_1, \gamma_2, \gamma_3) = (\gamma_1, 0, \gamma_3)$ , one non-Abelian axial vortex is attached by two domain walls. These two domain walls are attached from the opposite sides of the vortex. This vortex is unstable to decay into two chiral non-Abelian vortices introduced in Sec. V, each of which is attached by one domain wall.<sup>5</sup> See discussion in Sec. VII B.

If we turn on  $\gamma_2$ , how these two domain walls attach to the vortex depends on the parameters  $\gamma_1, \gamma_2$  as classified in Refs. [24,25] in the context of two-Higgs doublet models. In some case, these two domain walls constitute a composite wall. It is an open question whether the decay is suppressed or not in this case.

In terms of the gauge invariant  $\Sigma$  in Eq. (2.13), the ansatz in Eq. (4.4) can be rewritten as

$$\begin{aligned} -\Sigma &= \begin{pmatrix} F(r)e^{2i\varphi} & 0 \\ 0 & G(r)\mathbf{1}_{N-1} \end{pmatrix} \\ &= e^{\frac{2i}{N}\varphi} e^{\frac{i}{N}\varphi T_N} \begin{pmatrix} F(r) & 0 \\ 0 & G(r)\mathbf{1}_{N-1} \end{pmatrix} e^{\frac{i}{N}\varphi T_N} \\ &= e^{2i\theta_A(\varphi)} U(\varphi) \begin{pmatrix} F(r) & 0 \\ 0 & G(r)\mathbf{1}_{N-1} \end{pmatrix} U(\varphi), \end{aligned} \quad (4.8)$$

with  $F \equiv f^2$  and  $G = g^2$ , and  $U$  and  $\theta_A$  in Eq. (4.5). It is obvious that this vortex has a double-winding compared with the corresponding one in the linear sigma model. In fact, the one with unit winding in  $\Sigma$  discussed in Sec. 10 of the review paper [5] corresponds to the chiral non-Abelian vortex introduced in the next section.

## V. CHIRAL NON-ABELIAN VORTICES

In this section, we introduce a novel vortex of non-Abelian kind, that is, chiral non-Abelian vortices. Here, we restrict ourselves to the case in the absence of the chiral symmetry breaking terms:  $\gamma_1 = \gamma_2 = \gamma_3 = 0$  in which the axial and chiral symmetries become exact. We then discuss the topological obstruction and AB phases around these vortices.

### A. Solutions of chiral non-Abelian vortices

Chiral non-Abelian vortices introduced in this section are the minimum vortices in the CFL phase. There are two kinds of chiral non-Abelian vortices, namely of left and right chiralities, given by

$$\begin{aligned} \text{Left}(1, 0): \quad &\det \Phi_L \sim e^{i\varphi}, \det \Phi_R \sim 1, \\ \text{Right}(0, 1): \quad &\det \Phi_L \sim 1, \det \Phi_R \sim e^{i\varphi}, \end{aligned} \quad (5.1)$$

respectively. In order to construct these configurations, we note the relations for labels

$$\begin{aligned} (1, 0) &= \frac{1}{2}[(1, 1) + (1, -1)], \\ (0, 1) &= \frac{1}{2}[(1, 1) - (1, -1)]. \end{aligned} \quad (5.2)$$

These imply that a chiral non-Abelian vortex can be constructed as a sum of a half non-Abelian semisuperfluid vortex and a half non-Abelian axial vortex. We thus reach the ansatz for a chiral non-Abelian vortex of the left chirality  $(1, 0)$ , given in the polar coordinates  $(r, \varphi)$  by

<sup>5</sup>In the context of chiral symmetry breaking at low density, the axial vortex is attached by one domain wall [64], and decays do not occur.

$$\begin{aligned}
\Phi_L &= \begin{pmatrix} f(r)e^{i\varphi} & 0 \\ 0 & g(r)\mathbf{1}_{N-1} \end{pmatrix} \\
&= e^{\frac{i}{2N}\varphi} e^{\frac{i}{2N}\varphi} e^{\frac{i}{2N}\varphi T_N} \begin{pmatrix} f(r) & 0 \\ 0 & g(r)\mathbf{1}_{N-1} \end{pmatrix} e^{\frac{i}{2N}\varphi T_N} \\
&= e^{i\theta_B(\varphi)+i\theta_A(\varphi)} U(\varphi) \begin{pmatrix} f(r) & 0 \\ 0 & g(r)\mathbf{1}_{N-1} \end{pmatrix} U(\varphi), \\
-\Phi_R &= \begin{pmatrix} c(r) & 0 \\ 0 & d(r)\mathbf{1}_{N-1} \end{pmatrix} \\
&= e^{\frac{i}{2N}\varphi} e^{-\frac{i}{2N}\varphi} e^{\frac{i}{2N}\varphi T_N} \begin{pmatrix} c(r) & 0 \\ 0 & d(r)\mathbf{1}_{N-1} \end{pmatrix} e^{-\frac{i}{2N}\varphi T_N} \\
&= e^{i\theta_B(\varphi)-i\theta_A(\varphi)} U(\varphi) \begin{pmatrix} c(r) & 0 \\ 0 & d(r)\mathbf{1}_{N-1} \end{pmatrix} U^\dagger(\varphi) \\
A_i &= -\epsilon_{ij} \frac{x^j}{2Ng_s r^2} (1-h(r)) T_N \quad (5.3)
\end{aligned}$$

with

$$\begin{aligned}
e^{i\theta_B(\varphi)} &= e^{i\varphi/2N}, & e^{i\theta_A(\varphi)} &= e^{i\varphi/2N}, \\
(g_C = U_L^\dagger = U_R) U(\varphi) &= e^{\frac{i}{2N}\varphi T_N}. \quad (5.4)
\end{aligned}$$

The equations of motion for the profile functions are given by

$$\begin{aligned}
f'' + \frac{f'}{r} - \frac{((N-1)h + (N+1))^2}{4N^2 r^2} f + \frac{m^2}{2} f \\
- \frac{1}{2} [(\lambda_1 + \lambda_2)f^2 + (N-1)\lambda_2 g^2 + \lambda_3 c^2 \\
+ (N-1)\lambda_3 d^2] f = 0, \quad (5.5)
\end{aligned}$$

$$\begin{aligned}
g'' + \frac{g'}{r} - \frac{(h-1)^2}{4N^2 r^2} g + \frac{m^2}{2} g \\
- \frac{1}{2} [\lambda_2 f^2 + (\lambda_1 + (N-1)\lambda_2)g^2 + \lambda_3 c^2 \\
+ (N-1)\lambda_3 d^2] g = 0, \quad (5.6)
\end{aligned}$$

$$\begin{aligned}
c'' + \frac{c'}{r} - \frac{(N-1)^2(h-1)^2}{4N^2 r^2} c + \frac{m^2}{2} c \\
- \frac{1}{2} [\lambda_3 f^2 + (N-1)\lambda_3 g^2 + (\lambda_1 + \lambda_2)c^2 \\
+ (N-1)\lambda_2 d^2] c = 0, \quad (5.7)
\end{aligned}$$

$$\begin{aligned}
d'' + \frac{d'}{r} - \frac{(h-1)^2}{4N^2 r^2} d + \frac{m^2}{2} d \\
- \frac{1}{2} [\lambda_3 f^2 + (N-1)\lambda_3 g^2 + \lambda_2 c^2 \\
+ (\lambda_1 + (N-1)\lambda_2)d^2] d = 0, \quad (5.8)
\end{aligned}$$

$$\begin{aligned}
h'' - \frac{h'}{r} - \frac{2g_s^2}{N} [((N-1)f^2 + g^2 + (N-1)c^2 + d^2)h \\
+ (N+1)f^2 - g^2 - (N-1)c^2 - d^2] = 0. \quad (5.9)
\end{aligned}$$

The boundary condition is

$$\begin{aligned}
(f, g, c', d', h)_{r=0} &= (0, 0, 0, 0, 1), \\
(f, g, c, d, h)_{r=\infty} &= (v, v, v, v, 0). \quad (5.10)
\end{aligned}$$

Numerical solutions for several typical parameter combinations in the case of  $N=3$  are plotted in Fig. 1.

Compared with the ansatz for the usual non-Abelian semisuperfluid vortex in Eq. (3.2), the  $U(1)_B$  and  $SU(3)_C$  actions are halves of those of the ansatz in Eq. (3.2) winding in the sub-OPM  $\mathcal{M}_V = U(N)_{C-(L+R)+B}$ , and the rests are complemented by going through the other sub-OPM  $\mathcal{M}_A = U(N)_{L-R+A}$  for the axial and chiral symmetry breakings, which are halves of non-Abelian axial vortices in Eq. (4.4). A closed loop surrounding the chiral non-Abelian vortex is mapped onto a closed loop in the full OPM  $\mathcal{M}$  given in Eq. (2.8), and consequently, this carries  $1/2N$   $U(1)_B$  circulation and the color magnetic flux, both of which are halves of those of the usual non-Abelian semisuperfluid vortex. The color magnetic flux is  $1/2N$  of that of a pure color flux tube.

In the above ansatz in Eq. (5.3), we have considered the winding in the (1, 1) component. Instead, we can embed it in other diagonal components, thus finding  $N$  solutions of the same energy, as the case of the usual non-Abelian semisuperfluid vortex. Again, more generally, the  $SU(N)_{C+L+R}$  transformation on the ansatz in Eq. (5.3) yields a continuous family of solutions, again characterized by the moduli space

$$\mathbb{C}P^{N-1} = \frac{SU(N)_{C+L+R}}{SU(N-1) \times U(1)}. \quad (5.11)$$

Likewise, we also can construct a vortex of the right chirality (0, 1) winding in  $\Phi_R$  in the same way:

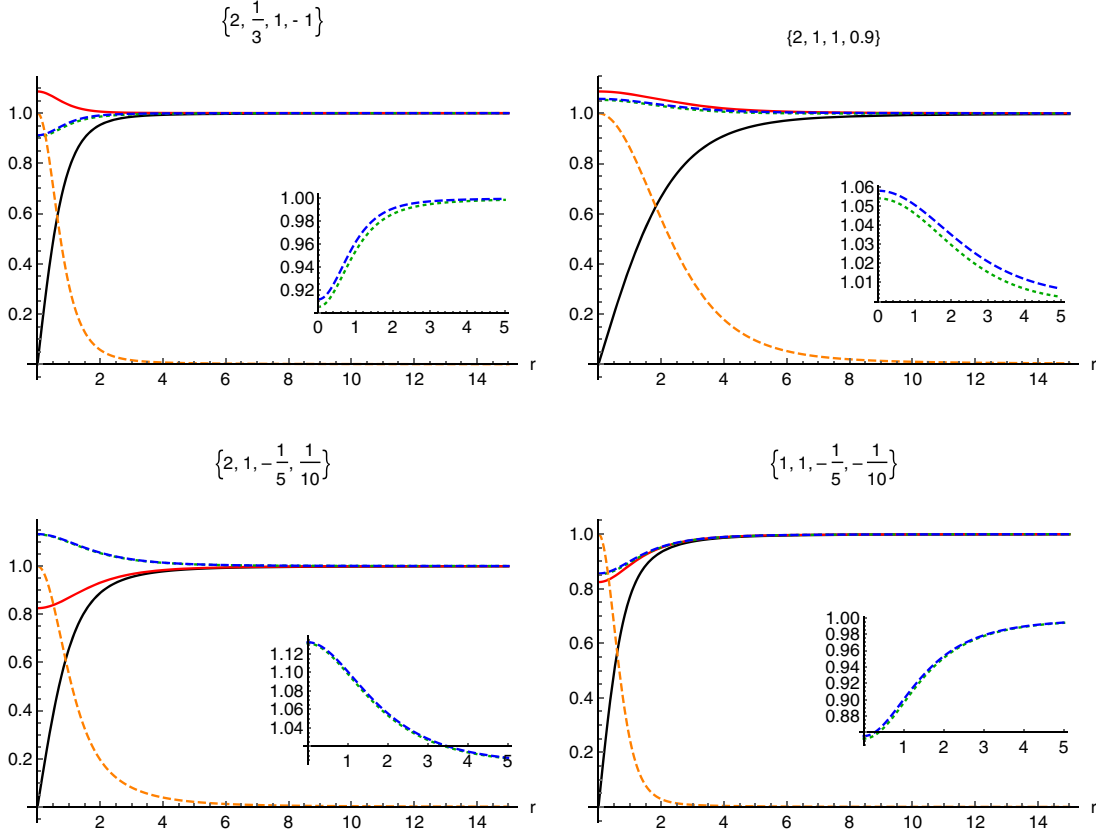


FIG. 1. Numerical solutions of a single left (right) chiral non-Abelian vortex for  $N = 3$ . The black-solid, red-solid, green-dotted, blue-dashed, and orange-dashed lines correspond to  $f(r)$ ,  $g(r)$ ,  $c(r)$ ,  $d(r)$ , and  $h(r)$ , respectively. The label at top of each panel shows the parameter combination  $\{m, \lambda_1, \lambda_2, \lambda_3\}$ . The profiles  $c(r)$  and  $d(r)$  are almost degenerate for all the cases, and the insets show small deviation between  $c(r)$  and  $d(r)$  near the origin.

$$\begin{aligned}
 \Phi_L &= \begin{pmatrix} c(r) & 0 \\ 0 & d(r)\mathbf{1}_{N-1} \end{pmatrix} \\
 &= e^{\frac{i}{2N}\varphi} e^{-\frac{i}{2N}\varphi} e^{\frac{i}{2N}\varphi T_N} \begin{pmatrix} c(r) & 0 \\ 0 & d(r)\mathbf{1}_{N-1} \end{pmatrix} e^{-\frac{i}{2N}\varphi T_N} \\
 &= e^{i\theta_B(\varphi) + i\theta_A(\varphi)} U(\varphi) \begin{pmatrix} c(r) & 0 \\ 0 & d(r)\mathbf{1}_{N-1} \end{pmatrix} U^\dagger(\varphi) \\
 -\Phi_R &= \begin{pmatrix} f(r)e^{i\varphi} & 0 \\ 0 & g(r)\mathbf{1}_{N-1} \end{pmatrix} \\
 &= e^{\frac{i}{2N}\varphi} e^{\frac{i}{2N}\varphi} e^{\frac{i}{2N}\varphi T_N} \begin{pmatrix} f(r) & 0 \\ 0 & g(r)\mathbf{1}_{N-1} \end{pmatrix} e^{\frac{i}{2N}\varphi T_N} \\
 &= e^{i\theta_B(\varphi) - i\theta_A(\varphi)} U(\varphi) \begin{pmatrix} f(r) & 0 \\ 0 & g(r)\mathbf{1}_{N-1} \end{pmatrix} U(\varphi), \\
 A_i &= -\epsilon_{ij} \frac{x^j}{2Ng_s r^2} (1 - h(r)) T_N, \quad (5.12)
 \end{aligned}$$

with the same profile functions as those in Eq. (5.3) and the same boundary conditions for them with Eq. (5.10). This carries the same  $U(1)_B$  circulation and the same color magnetic flux with those with the left one in Eq. (5.3), but

the  $U(1)_A$  and  $SU(N)_{L-R}$  transformations are opposite to those of the left one in Eq. (5.3):

$$\begin{aligned}
 e^{i\theta_B(\varphi)} &= e^{i\varphi/2N}, & e^{i\theta_A(\varphi)} &= e^{-i\varphi/2N}, \\
 (g_C = U_L = U_R^\dagger) U(\varphi) &= e^{\frac{i}{2N}\varphi T_N}. \quad (5.13)
 \end{aligned}$$

A continuous family of solutions is parametrized by a copy of the moduli space in Eq. (5.11).

In terms of the gauge invariant  $\Sigma$  in Eq. (2.13), the chiral non-Abelian vortex of the left chirality (1, 0) in Eq. (5.3) can be rewritten as

$$\begin{aligned}
 -\Sigma &= \begin{pmatrix} F(r)e^{+i\varphi} & 0 \\ 0 & G(r)\mathbf{1}_{N-1} \end{pmatrix} \\
 &= e^{\frac{i}{2N}\varphi} e^{-\frac{i}{2N}\varphi T_N} \begin{pmatrix} F(r) & 0 \\ 0 & G(r)\mathbf{1}_{N-1} \end{pmatrix} e^{-\frac{i}{2N}\varphi T_N} \\
 &= e^{2i\theta_A(\varphi)} U(\varphi) \begin{pmatrix} F(r) & 0 \\ 0 & G(r)\mathbf{1}_{N-1} \end{pmatrix} U(\varphi), \quad (5.14)
 \end{aligned}$$

with  $F \equiv fc$ ,  $G \equiv gd$ , and  $U(\varphi)$  and  $e^{2i\theta_A(\varphi)}$  in Eq. (5.4), while the one of the right chirality (0, 1) in Eq. (5.12) can be rewritten as

$$\begin{aligned}
-\Sigma &= \begin{pmatrix} F(r)e^{-i\varphi} & 0 \\ 0 & G(r)\mathbf{1}_{N-1} \end{pmatrix} \\
&= e^{-\frac{i}{N}\varphi} e^{-\frac{i}{2N}\varphi T_N} \begin{pmatrix} F(r) & 0 \\ 0 & G(r)\mathbf{1}_{N-1} \end{pmatrix} e^{-\frac{i}{2N}\varphi T_N} \\
&= e^{2i\theta_A(\varphi)} U^\dagger(\varphi) \begin{pmatrix} F(r) & 0 \\ 0 & G(r)\mathbf{1}_{N-1} \end{pmatrix} U^\dagger(\varphi), \quad (5.15)
\end{aligned}$$

with  $F \equiv fc$ ,  $G \equiv gd$ , and  $U(\varphi)$  and  $e^{2i\theta_A(\varphi)}$  in Eq. (5.13). These two just look like an antivortex to each other. In other words, vortices labeled by  $(1, 0)$  and  $(0, -1)$  have the same form of  $\Sigma$ . However, the vortices  $(1, 0)$  and  $(0, -1)$  are distinct because the color magnetic fluxes that they carry are opposite to each other, which are invisible in  $\Sigma$ .

With this regards, vortices in the linear sigma model in terms of  $\Sigma$  discussed in Sec. 10 of the review paper [5] actually describe chiral non-Abelian vortices discussed in this section and should carry magnetic fluxes (invisible in the linear sigma model), although this fact was not recognized in Ref. [5].

## B. Topological obstruction

Here we discuss the so-called topological obstruction (see Appendix A 4 for its definition) common for the vortices with the left and right chiralities in Eqs. (5.3) and (5.12). If we encircle the vortex, the generators  $T_A$  ( $A = 1, \dots, N^2 - 1$ ) of the  $SU(N)_C$  gauge group transform accordingly as

$$\begin{aligned}
T_A(\varphi) &\equiv U(\varphi)T_A U^\dagger(\varphi) \\
&= \exp\left[\frac{i\varphi}{2N}\text{diag.}(N-1, -1, \dots, -1)\right] T_A \\
&\quad \times \exp\left[-\frac{i\varphi}{2N}\text{diag.}(N-1, -1, \dots, -1)\right] \\
&= \left(\begin{array}{c|c} (T_A)_{ij} & e^{+i\varphi/2}(T_A)_{1j} \\ \hline e^{-i\varphi/2}(T_A)_{i1} & (T_A)_{ij} \end{array}\right) \quad (5.16)
\end{aligned}$$

with  $i, j = 2, \dots, N$ . After complete encirclement ( $\varphi = 2\pi$ ), these become

$$\begin{aligned}
Q_L &\rightarrow \exp\left[-\frac{i\pi}{N}\text{diag.}(N-1, -1, \dots, -1)\right] Q_L = \text{diag.}(\epsilon^{-N+1}, \epsilon, \dots, \epsilon) Q_L, \\
Q_R &\rightarrow \exp\left[-\frac{i\pi}{N}\text{diag.}(N-1, -1, \dots, -1)\right] Q_R = \text{diag.}(\epsilon^{-N+1}, \epsilon, \dots, \epsilon) Q_R, \quad (5.20)
\end{aligned}$$

with  $\epsilon$  is the  $2N$ -th root of the unity,

$$\epsilon = \exp(\pi i/N), \quad (\epsilon^{2N} = 1). \quad (5.21)$$

These form a  $\mathbb{Z}_{2N}$  group. This is a color nonsinglet, implying that heavy quarks can detect the color of the magnetic flux of the vortex from infinite distances. Note that, after two successive encirclements ( $\varphi = 4\pi$ ), they become

$$T_A(\varphi = 2\pi) = \left(\begin{array}{c|c} (T_A)_{11} & -(T_A)_{1j} \\ \hline -(T_A)_{i1} & (T_A)_{ij} \end{array}\right) \neq T_A(\varphi = 0), \quad (5.17)$$

implying that the off-diagonal blocks are not single-valued around the vortex. Those off-diagonal blocks correspond to the broken generators of the  $\mathbb{C}P^{N-1}$  moduli in Eq. (5.11). This phenomenon is known as the topological obstruction. More precisely, the obstruction is present for the CFL symmetry in Eq. (2.7) rather than the gauge symmetry itself.

The two complete encirclements give

$$T_A(\varphi = 4\pi) = T_A(\varphi = 0). \quad (5.18)$$

This also implies that there is no obstruction around the usual non-Abelian semisuperfluid vortex in Eq. (3.2).

For vortices with different color magnetic fluxes corresponding to the  $\mathbb{C}P^{N-1}$  moduli in Eq. (5.11), corresponding broken generators have the obstruction.

## C. Generalized Aharonov-Bohm phases

AB phases around the usual non-Abelian semisuperfluid vortices were studied for the electromagnetism [79], and for color gauge field [37–39]. Here, we do not consider electromagnetism. Let us discuss generalized AB phases around a single chiral non-Abelian vortex. In the CFL phase ( $N = 3$ ), the light quarks  $q$  and heavy quarks  $Q$  receive the following transformations from Eqs. (5.3) and (5.4) when they encircle the vortex.

The heavy quarks not participating condensations receive ordinary AB phases contributed only from the gauge symmetry as

$$\begin{aligned}
Q_L &\rightarrow g_C^*(\varphi) Q_L = \exp\left[-\frac{i\varphi}{2N}\text{diag.}(N-1, -1, \dots, -1)\right] Q_L, \\
Q_R &\rightarrow g_C^*(\varphi) Q_R = \exp\left[-\frac{i\varphi}{2N}\text{diag.}(N-1, -1, \dots, -1)\right] Q_R. \quad (5.19)
\end{aligned}$$

After complete encirclement ( $\varphi = 2\pi$ ), these phases become

$$\begin{aligned} Q_L &\rightarrow \text{diag.}(\epsilon^{-2N+2}, \epsilon^2, \dots, \epsilon^2) Q_L = \epsilon^2 Q_L, \\ Q_R &\rightarrow \text{diag.}(\epsilon^{-2N+2}, \epsilon^2, \dots, \epsilon^2) Q_R = \epsilon^2 Q_R. \end{aligned} \quad (5.22)$$

Thus, even numbers of manipulations give a  $\mathbb{Z}_N$  group, which is a color singlet.

On the other hand, the light quarks participate condensations, thus receiving generalized AB phases consisting of two contributions from the vortex winding and AB phases purely coming from the color gauge group, as was studied for usual non-Abelian semisuperfluid vortices in the CFL phase [37,38] as well as non-Abelian Alice strings in the  $2SC+\langle dd \rangle$  phase [68–70] (see Appendix C). In our case, generalized AB phases around a chiral non-Abelian vortex are

$$\begin{aligned} q_L &\rightarrow e^{i\theta_B(\varphi)/2} e^{i\theta_A(\varphi)/2} g_C^*(\varphi) q_L U_L^T(\varphi) \\ &= e^{i\varphi/2N} \exp \left[ -\frac{i\varphi}{2N} \text{diag.}(N-1, -1, \dots, -1) \right] q_L \\ &\quad \exp \left[ -\frac{i\varphi}{2N} \text{diag.}(N-1, -1, \dots, -1) \right] \\ &= \left( \begin{array}{c|c} e^{-i((2N-3)/2N)\varphi} (q_L)_{11} & e^{-i((N-3)/2N)\varphi} (q_L)_{1j} \\ \hline e^{-i((N-3)/2N)\varphi} (q_L)_{i1} & e^{i(3/2N)\varphi} (q_L)_{ij} \end{array} \right), \\ q_R &\rightarrow e^{i\theta_B(\varphi)/2} e^{-i\theta_A(\varphi)/2} g_C^*(\varphi) q_R U_R^T(\varphi) \\ &= \exp \left[ -\frac{i\varphi}{2N} \text{diag.}(N-1, -1, \dots, -1) \right] q_R \\ &\quad \exp \left[ +\frac{i\varphi}{2N} \text{diag.}(N-1, -1, \dots, -1) \right] \\ &= \left( \begin{array}{c|c} (q_R)_{11} & e^{-i\varphi/2} (q_R)_{1j} \\ \hline e^{+i\varphi/2} (q_R)_{i1} & (q_R)_{ij} \end{array} \right) \end{aligned} \quad (5.23)$$

with  $i, j = 2, \dots, N$ . After complete encirclement ( $\varphi = 2\pi$ ), they become

$$\begin{aligned} q_L &\rightarrow \left( \begin{array}{c|c} e^{-((2N-3)/N)\pi i} (q_L)_{11} & e^{-i((N-3)/N)\pi i} (q_L)_{1j} \\ \hline e^{-i((N-3)/N)\pi i} (q_L)_{i1} & e^{3\pi i/N} (q_L)_{ij} \end{array} \right) \\ &= \left( \begin{array}{c|c} -(q_L)_{11} & (q_L)_{1j} \\ \hline (q_L)_{i1} & -(q_L)_{ij} \end{array} \right) \quad (\text{for } N=3), \\ q_R &\rightarrow \left( \begin{array}{c|c} (q_R)_{11} & -(q_R)_{1j} \\ \hline -(q_R)_{i1} & (q_R)_{ij} \end{array} \right). \end{aligned} \quad (5.24)$$

For the case of  $N=3$ , even numbers of encirclements give a trivial action.

## VI. ENERGETICS OF VORTICES

In this section, we calculate the leading contributions to tensions of vortices, in particular of chiral non-Abelian vortices  $(1, 0)$  and  $(0, \pm 1)$ , non-Abelian semisuperfluid vortices  $(1, 1)$ , and non-Abelian axial vortices  $(1, -1)$ . We

also calculate the tension of a composite state of two chiral non-Abelian vortices  $(1, 0)$  and  $(0, 1)$  with different  $\mathbb{C}P^{N-1}$  orientations, to show that these orientations are energetically favored to be aligned to each other, while  $\mathbb{C}P^{N-1}$  orientations of two chiral non-Abelian vortices  $(1, 0)$  and  $(0, -1)$  are energetically favored to be orthogonal to each other.

### A. Two vortices with parallel $\mathbb{C}P^{N-1}$ orientations

Since all vortices discussed in this model have global  $U(1)_B$  windings, the leading contributions to their tensions are logarithmically divergent with coming from the kinetic term of  $\Phi_{R,L}$ , as usual for global vortices.

We consider the following asymptotic configuration characterized by a set of two integers  $\{k_L, k_R\}$ :

$$\Phi_L \rightarrow v \text{diag.} (e^{ik_L\varphi}, 1, \dots, 1), \quad (6.1)$$

$$\Phi_R \rightarrow v \text{diag.} (e^{ik_R\varphi}, 1, \dots, 1), \quad (6.2)$$

as  $r \rightarrow \infty$ . We have taken the  $\mathbb{C}P^{N-1}$  moduli of the  $(1, 0)$  vortex of the left chirality to be oriented to the first component without loss of generality, and we assume that of the  $(0, 1)$  vortex of the right chirality to be aligned to the  $(1, 0)$  vortex in this subsection. The case that they are not aligned is discussed in the next subsection.

The gauge fields should be chosen in such a way that the kinetic energy of  $\Phi_{L,R}$  is minimized:

$$A_i \rightarrow -\epsilon_{ij} \frac{(k_L + k_R)x^j}{2Ng_s r^2} T_N. \quad (6.3)$$

Then, the scalar kinetic energy reads

$$\begin{aligned} \mathcal{K} &= \text{Tr}[\mathcal{D}_i \Phi_L^\dagger \mathcal{D}_i \Phi_L + \mathcal{D}_i \Phi_R^\dagger \mathcal{D}_i \Phi_R] \\ &\rightarrow \frac{v^2 N + 1}{r^2} \frac{1}{2N} F_N(k_L, k_R), \end{aligned} \quad (6.4)$$

where  $F_N$  is given by

$$\begin{aligned} F_N(k_L, k_R) &= k_L^2 - \frac{2(N-1)}{N+1} k_L k_R + k_R^2 \\ &= (k_L - k_R)^2 + \frac{4}{N+1} k_L k_R. \end{aligned} \quad (6.5)$$

We thus find that the leading term of the tension is given by

$$K = 2\pi \int^\Lambda dr r \mathcal{K} = \frac{(N+1)\pi v^2}{N} F_N(k_L, k_R) \log \Lambda, \quad (6.6)$$

where  $\Lambda$  is an IR cutoff parameter, or the size of the system.

We have  $F_N(1, 0) = F_N(0, 1) = 1$  for a single chiral non-Abelian vortex  $(1, 0)$  or  $(0, 1)$ , and  $F_N(1, 1) = 4/(N+1)$  for a single non-Abelian semisuperfluid vortex  $(1, 1)$ . Comparing these two, we find  $F_N(1, 0) < F_N(1, 1)$

for  $N \leq 2$ ,  $F_N(1, 0) = F_N(1, 1)$  for  $N = 3$  (relevant to QCD), and  $F_N(1, 0) > F_N(1, 1)$  for  $N \geq 4$ .

By using these results, we can discuss whether two separated chiral non-Abelian vortices with the opposite chiralities (1, 0) and (0, 1) are energetically bound to a single non-Abelian semisuperfluid vortex (1, 1) or not. To this end, we note that when the vortices (1, 0) and (0, 1) are infinitely separated, the tension of such a composite state is proportional to a sum of the tensions of individual vortices:  $F_N(1, 0) + F_N(0, 1) = 2$ . Comparing this with  $F_N(1, 1)$  of a single non-Abelian semisuperfluid vortex, we find

$$F_N(1, 0) + F_N(0, 1) (= 2) \begin{cases} = F_N(1, 1) = 2 & \text{for } N = 1 \\ > F_N(1, 1) = \frac{4}{N+1} & \text{for } N \geq 2 \end{cases} \quad (6.7)$$

This implies that two chiral non-Abelian vortices with the opposite chiralities (1, 0) and (0, 1) attract each other for  $N \geq 2$ , while there is no force between them at this order for  $N = 1$ . The latter corresponds to two-component BECs in which the absence of the leading order interaction is in fact known [76].

In a similar way, we can discuss the stability of a non-Abelian axial vortex (1, -1). When the vortices (1, 0) and (0, -1) are infinitely separated, the tension of such a composite state is proportional to  $F_N(1, 0) + F_N(0, -1) = 2$ . Comparing this with  $F_N(1, -1) = 4N/(N+1)$  of a single non-Abelian axial vortex, we find

$$F_N(1, 0) + F_N(0, -1) (= 2) \begin{cases} = F_N(1, -1) = 2 & \text{for } N = 1 \\ < F_N(1, -1) = \frac{4N}{N+1} & \text{for } N \geq 2 \end{cases}, \quad (6.8)$$

implying that two chiral non-Abelian vortices with the opposite chiralities (1, 0) and (0, -1) repel each other for  $N \geq 2$ , while there is no force between them at this order for  $N = 1$ . We thus have found that for  $N \geq 2$  the non-Abelian axial vortex (1, -1) is unstable to decay into (1, 0) and (0, -1) chiral non-Abelian vortices.

### B. Two vortices with orthogonal $\mathbb{C}P^{N-1}$ orientations

In this subsection, we take the  $\mathbb{C}P^{N-1}$  moduli of the (1, 0) and (0, 1) vortices to be orthogonal to each other, which is possible for  $N \geq 2$ . To this end, without loss of generality, we consider the following asymptotic configuration characterized by the set of two integers  $\{k_L, k_R\}$ ,

$$\Phi_L \rightarrow v \text{diag} (e^{ik_L \varphi}, 1, \dots, 1), \quad (6.9)$$

$$\Phi_R \rightarrow v \text{diag} (1, e^{ik_R \varphi}, \dots, 1), \quad (6.10)$$

as  $r \rightarrow \infty$ . In this case, the gauge fields should be chosen in such a way that the kinetic energy of  $\Phi_{L,R}$  is minimized:

$$A_i \rightarrow -\epsilon_{ij} \frac{k_L x^j}{2Ng_s r^2} T_N - \epsilon_{ij} \frac{k_R x^j}{2Ng_s r^2} T'_N, \quad (6.11)$$

with  $T'_N = \text{diag}(-1, N-1, -1, \dots, -1)$ . Then, the scalar kinetic energy reads

$$\mathcal{K} \rightarrow \frac{v^2 N + 1}{r^2} G_N(k_L, k_R), \quad (6.12)$$

with  $G$  defined by

$$G_N(k_L, k_R) = k_L^2 + \frac{1}{N+1} k_L k_R + k_R^2. \quad (6.13)$$

Thus, the leading contribution to the tension of the composite state can be calculated, to give

$$K = 2\pi \int^\Lambda dr r \mathcal{K} = \frac{(N+1)\pi v^2}{N} G_N(k_L, k_R) \log \Lambda. \quad (6.14)$$

The tension of a set of two non-Abelian chiral vortices (1, 0) and (0, 1) with the  $\mathbb{C}P^{N-1}$  orientations orthogonal to each other is thus found to be proportional to  $G_N(1, 1) = 2 + 1/(N+1)$ . Since we have an inequality

$$F_N(1, 1) = \frac{4}{N+1} < G_N(1, 1) = 2 + \frac{1}{N+1} \quad (6.15)$$

for all  $N(\geq 2)$ , the chiral non-Abelian vortices with aligned  $\mathbb{C}P^{N-1}$  orientations are energetically more favored than those with orthogonal orientations, implying that their  $\mathbb{C}P^{N-1}$  moduli attract each other, to be aligned.

Again, in a similar way, we can discuss the case of two chiral non-Abelian vortices with the opposite chiralities (1, 0) and (0, -1). In this case, we have an inequality

$$F_N(1, -1) = \frac{4N}{N+1} > G_N(1, -1) = 2 - \frac{1}{N+1} \quad (6.16)$$

for all  $N(\geq 2)$ . Thus, two chiral non-Abelian vortices (1, 0) and (0, -1) with orthogonal  $\mathbb{C}P^{N-1}$  orientations are energetically more favored than those with aligned orientations, implying that their  $\mathbb{C}P^{N-1}$  moduli repel each other. If we separate them infinitely, the tension becomes  $G_N(1, 0) + G_N(0, -1) = 2$ . The inequality

$$G_N(1, 0) + G_N(0, -1) = 2 > G_N(1, -1) = 2 - \frac{1}{N+1} \quad (6.17)$$

implies that the two chiral non-Abelian vortices (1, 0) and (0, -1) with orthogonal  $\mathbb{C}P^{N-1}$  orientations attract each other, forming a bound state. It is, however, a highly nontrivial dynamical question remaining as a future problem.

## VII. VORTEX-DOMAIN WALL COMPOSITES

We consider the case of  $\gamma_1, \gamma_2, \gamma_3 \neq 0$  in which the axial and chiral symmetries are explicitly broken. This breaking induces domain walls attached to the vortices.

### A. Chiral non-Abelian vortices attached by chiral domain walls

Let us turn on  $\gamma_1, \gamma_2, \gamma_3 \neq 0$  to see their effects on vortices. In this subsection, we consider a chiral non-Abelian vortex. In Fig. 2, we present numerical simulations in the case that either of  $\gamma_1, \gamma_2, \gamma_3$  is nonzero. We can clearly see that one chiral non-Abelian vortex is attached by one or two domain walls. The three columns correspond from the left to the right to  $(\gamma_1, \gamma_2, \gamma_3) = (*, 0, 0), (0, *, 0), (0, 0, *)$ , respectively. In the middle column  $\gamma_2 \neq 0$ , the vortex is attached by the two domain walls with the same tension, and thus the configuration is stable. In left-most and right-most cases, the vortex is attached by one domain wall from one side. The wall pulls the vortex and the configuration is unstable, but it is static in the comoving frame.

To see why this happens, we consider an infinitely large circle parametrized by the spatial angle  $\varphi$  encircling vortices. Let us substitute the chiral non-Abelian vortex ansatz of either the left chirality in Eq. (5.3) or the right chirality in Eq. (5.12) to the potential term in Eq. (2.5), with replacing the spatial angle  $\varphi$  by a function  $\phi(\varphi)$  depending on the angle  $\varphi$  with the boundary condition  $\phi(\varphi = 0) = 0$  and  $\phi(\varphi = 2\pi) = 2\pi$ . It can be evaluated at spatial infinities as

$$V = 2(\gamma_1 + \gamma_3) \cos \phi(\varphi) + 2\gamma_2 \cos(2\phi(\varphi)). \quad (7.1)$$

Together with the gradient term, the effective energy for  $\phi$  on the large circle at infinity encircling the chiral non-Abelian axial vortex becomes  $\mathcal{E}_{\text{eff}} = v^2(\partial_\varphi \phi)^2 + V$ . This is the double sine-Gordon model. Note that the periodicity is  $2\pi$  in contrast to the case of non-Abelian axial vortices in Eq. (4.7) in which the periodicity was  $\pi$ .

First, let us consider the absence of  $\gamma_3$  ( $\gamma_3 = 0$ ). The case of  $(\gamma_1, \gamma_2, \gamma_3) = (\gamma_1, 0, 0)$  corresponds to the sine-Gordon model, the case of  $(\gamma_1, \gamma_2, \gamma_3) = (0, \gamma_2, 0)$  to the sine-Gordon model with a half periodicity, and the case of  $(\gamma_1, \gamma_2, \gamma_3) = (\gamma_1, \gamma_2, 0)$  to the double sine-Gordon model. In the first case, a single chiral non-Abelian vortex is attached by a single sine-Gordon soliton, and thus is confined as shown in Figs. 2(a1)–2(a7). In the second case, it is attached by two sine-Gordon solitons (or domain walls) of the same tension from the opposite sides, and therefore the composite state is stable, see Figs. 2(b1)–2(b7). This case is a non-Abelian generalization of chiral P-wave superconductors, for which the GL theory is described by a  $U(1)$  gauge theory coupled with two complex scalar fields  $\Phi_1$  and  $\Phi_2$  with a potential term  $V \sim (\Phi_1^*)^2(\Phi_2)^2 + \text{c.c.}$  [80,81]. In the third case, it is

attached by two sine-Gordon solitons (or domain walls), but how they attach depends on the parameters  $\gamma_1, \gamma_2$  as classified in Refs. [24,25] in the context of two Higgs doublet models. In these cases, the domain walls attached to the chiral non-Abelian vortex are non-Abelian sine-Gordon solitons carrying  $\mathbb{C}P^{N-1}$  moduli [82,83]. This can be clearly seen in Fig. 2; The component  $\Phi_L^{11}$  has the vortex winding [(a1) and (b1)]. If one looks at the right condensation along the domain wall, one finds that  $\Phi_R^{11}$  is concave [Figs. 2(a3) and 2(b3)] while  $\Phi_R^{22}$  and  $\Phi_R^{33}$  are convex [Figs. 2(a4) and 2(b4)]. The same happens in the left condensations along the wall far apart from the vortex [Figs. 2(a1), 2(a2), 2(b1), and 2(b2)]. Thus, the  $SU(3)$  symmetry is spontaneously broken down to  $SU(2) \times U(1)$  along the domain wall, resulting in the  $\mathbb{C}P^2$  NG modes localized on the wall or attributing the  $\mathbb{C}P^2$  moduli. These moduli match those in Eq. (5.11) of the vortex along the junction line of the vortex and domain walls.

When only  $\gamma_3$  is present,  $(\gamma_1, \gamma_2, \gamma_3) = (0, 0, \gamma_3)$ , one sine-Gordon soliton is attached to one chiral non-Abelian vortex as shown in Fig. 2(c1)–(c7). This is Abelian, carrying no moduli. Indeed, the profile functions  $|\Phi_{L,R}^{(i,i)}|^2$  behave almost the same along the domain wall far from the vortex core. This implies that  $\Phi_{L,R}$  are proportional to the identity, and so no symmetries are broken by the domain wall.

When all  $\gamma_{1,2,3}$  are present, there appears either attraction or repulsion among the domain walls attached to the vortex, depending on its sign. If it is attraction, the domain walls form a composite domain wall [5,54], thus confining the chiral non-Abelian vortex. If repulsion, the chiral non-Abelian vortex is attached by two domain walls with different tensions from opposite sides. Such details of the domain wall structure are worth studying on their own, but are not relevant in the following subsections for vortex molecules, as explained below.

If we do the same for the usual non-Abelian semi-superfluid vortex in Eq. (3.2), there is no potential term, implying that no domain wall is attached to the usual non-Abelian semisuperfluid vortex.

### B. Decay of Abelian and non-Abelian axial vortices

Here we discuss that Abelian and non-Abelian axial vortices are all unstable to decay into a set of chiral non-Abelian vortices once the axial and chiral symmetry breaking terms are turned on.

One non-Abelian axial vortex discussed in Sec. IV B is attached from the opposite sides by two [or four for  $(\gamma_1, \gamma_2, \gamma_3) = (0, \gamma_2, 0)$ ] domain walls extending to infinities, and thus decays into two chiral non-Abelian vortices each of which is attached by one (or two) chiral domain wall(s) as in Fig. 3(a); one of the left chirality and the other of the right chirality with the opposite winding. This decay process can be written as

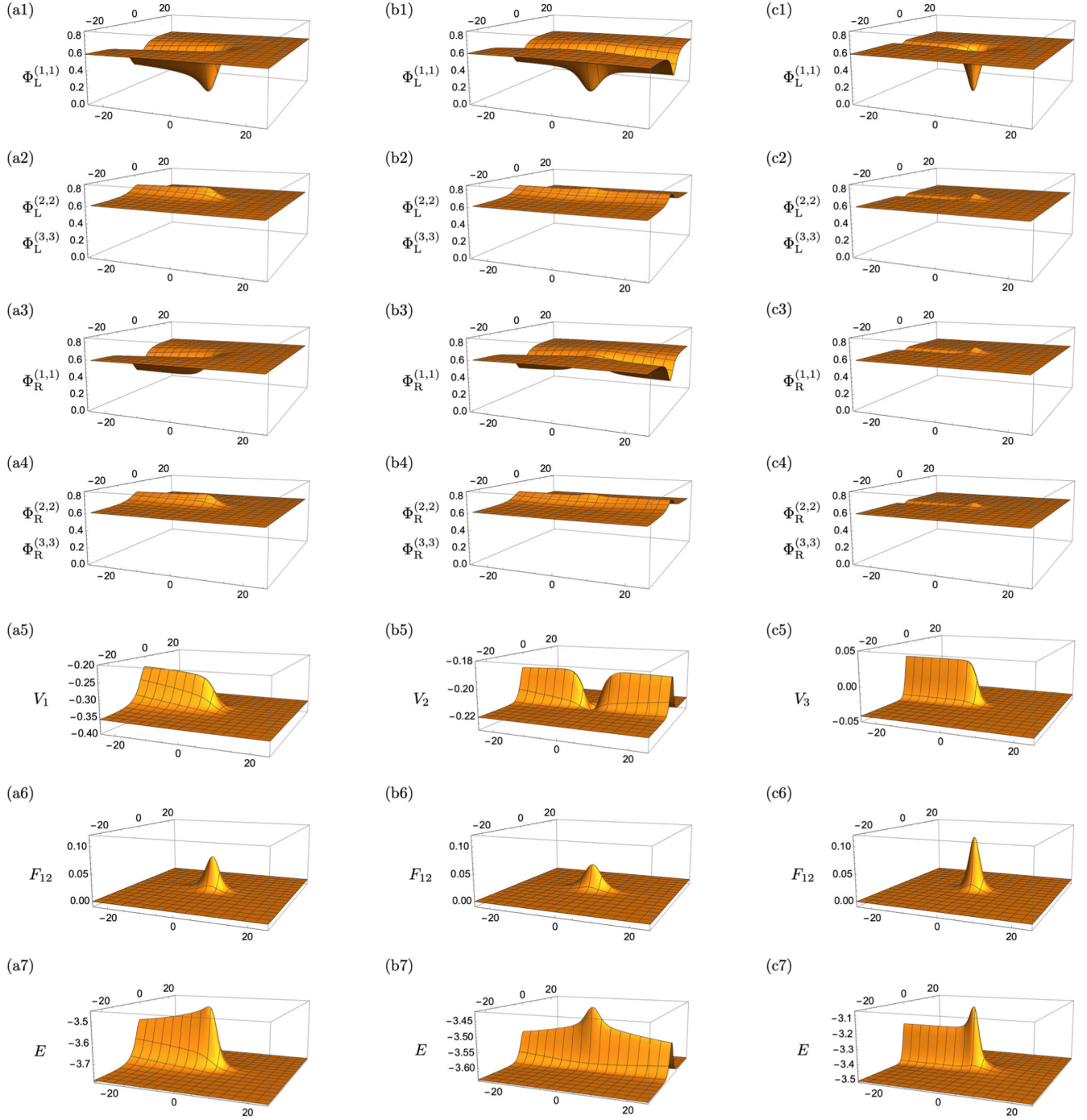


FIG. 2. The profile functions  $|\Phi_{L,R}^{(i,i)}|^2$  ( $i = 1, 2, 3$ ) of the vortex-wall composites. The left-most, middle, and right-most columns have  $(\gamma_1, \gamma_2, \gamma_3) = (-0.1, 0, 0), (0, -0.1, 0), (0, 0, -0.2)$ , respectively. The other parameters are common for all cases as  $(m, \lambda_1, \lambda_2, \lambda_3, \lambda_4, g) = (\sqrt{2}, 1, 1, 1, 0, 1)$ .

$$(1, -1) \rightarrow (1, 0) + (0, -1). \quad (7.2) \quad (N, -N) \rightarrow N(1, -1) \rightarrow N(1, 0) + N(0, -1). \quad (7.3)$$

It is interesting to observe that there was no flux in the initial state while the final states contain fluxes. Similarly, the Abelian axial vortex is also unstable to decay as

Another example is a doubly-wound chiral non-Abelian vortex with the same chirality, say left. This is also attached by two [or four for  $(\gamma_1, \gamma_2, \gamma_3) = (0, \gamma_2, 0)$ ] chiral domain

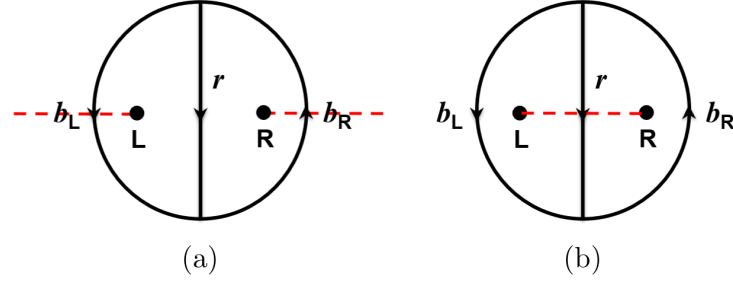


FIG. 3. Pairs of chiral non-Abelian vortices (a) attached by domain walls extending to infinities, leading to the instability against a decay, and (b) forming a chiral non-Abelian vortex molecule connected by a domain wall. For both cases, left (right) chiral non-Abelian vortices placed at L and R are encircled by the closed loops  $b_L - r$  and  $b_R + r$ , respectively. (a) They have the opposite windings  $(1, 0)$  and  $(0, -1)$ , and are attached by domain walls extending to infinities, leading the instability against decay. (b) These vortices have the same windings  $(1, 0)$  and  $(0, 1)$ , and are connected by a domain wall denoted by a red broken line to form a vortex molecule.

walls extending to infinities (but vortices of the same chirality are placed at both L and R), and therefore it is also unstable against decay into two chiral non-Abelian vortices each of which is attached by one (or two) chiral domain wall(s) as in Fig. 3(a). This decay process can be written as

$$(2, 0) \rightarrow 2(1, 0). \quad (7.4)$$

Similarly, an Abelian axial string having the minimum unit winding in  $\Sigma$  can decay as

$$(N, 0) \rightarrow N(1, 0). \quad (7.5)$$

This decay was numerically simulated in the linear sigma model [5,54].

## VIII. NON-ABELIAN VORTEX MOLECULES

### A. Structure of chiral non-Abelian vortex molecules

Before discussing the effect of explicit breaking terms  $\gamma_{1,2,3} \neq 0$  for general case, let us make a comment on the interaction between chiral non-Abelian vortices for  $\gamma_{1,2,3} = 0$  in the case of  $N = 1$ , in which the system reduces to two-component BECs. In this case, the interaction energy between  $(1, 0)$  and  $(\pm 1, 0)$  vortices at distance  $R$  is well known  $E_{\text{int}} \sim \pm \log R$ . Thus, a vortex and (anti)vortex repel (attract) each other as usual for single component global (superfluid) vortices. On the other hand, the interaction energy between  $(1, 0)$  and  $(0, 1)$  vortices at distance  $R$  vanishes at the leading order, to be consistent with Eq. (6.8), and the next leading order is  $E_{\text{int}} \sim \lambda \log R/R^2$  [76] with  $\lambda$  being  $\lambda_3$  and/or  $\lambda_4$  in Eq. (2.5) (reducing the same term for  $N = 1$ ). Thus, it can be either repulsive ( $\lambda > 0$ ) or attractive ( $\lambda < 0$ ). Once we introduce the explicit breaking terms  $\gamma_{1,2,3} \neq 0$ , a pair of  $(1, 0)$  and  $(0, 1)$  vortices forms a molecule in which constituents are separated at finite distance, when they are repulsive ( $\lambda > 0$ ) [48,51]. They collapse to form an Abelian vortex  $(1, 1)$  when they are attractive ( $\lambda < 0$ ).

Here, we show that the chiral non-Abelian vortices  $(1, 0)$  and  $(0, 1)$  can form a molecule. They have the same color magnetic fluxes. Now we put a  $(1, 0)$ -vortex on the left at ‘‘L’’ and a  $(0, 1)$ -vortex on the right at ‘‘R’’ in Fig. 3(b). We assume that the  $\mathbb{C}P^{N-1}$  orientations of these vortices are the same. The loop  $b_R + r$  encircles the  $(0, 1)$ -vortex while the one  $b_L - r$  encircles the  $(1, 0)$ -vortex. The large loop  $b_R + b_L$  encircles the both of them.

Along each of the large half circles  $b_L$  and  $b_R$ , the vector transformations, i.e., the color gauge transformation and  $U(1)_B$  transformation act as

$$b_L, b_R: g_C(\varphi) = e^{\frac{i}{2N}F(\varphi \mp \frac{\pi}{2})T_N}, \quad F(0) = 0, \quad F(\pi) = 2\pi \quad (8.1)$$

$$e^{i\theta_B(\varphi)} = e^{iB(\varphi \mp \frac{\pi}{2})}, \quad B(0) = 0, \quad B(\pi) = \pi/N, \quad (8.2)$$

respectively, where  $F$  and  $B$  are monotonically increasing functions (linear functions). On the other hand, along the path  $r$ , we have

$$r: U_L^\dagger = U_R = e^{\frac{i}{2N}R(y)T_N}, \quad R(-\infty) = 0, \quad R(+\infty) = 2\pi \quad (8.3)$$

$$e^{i\theta_A(y)} = e^{iA(y)}, \quad A(-\infty) = 0, \quad A(+\infty) = \pi/N, \quad (8.4)$$

respectively, where we have parametrized the path  $r$  by the coordinate  $y$ , and  $R$  and  $A$  are monotonically increasing functions.

Therefore, along the path  $r$ , there appears a (composite) domain wall stretching between the  $(1, 0)$ - and  $(0, 1)$ -vortices once  $\gamma_{1,2,3}$  are turned on. The internal structure of the domain wall depends on the values of  $\gamma_{1,2,3}$ , as discussed in Sec. VII A. In the presence of only  $\gamma_{1,3}$ , there exists one domain wall between the vortices, while there are two domain walls in the presence of  $\gamma_2$ . Nevertheless, all domain walls must be stretched between the two vortices since there

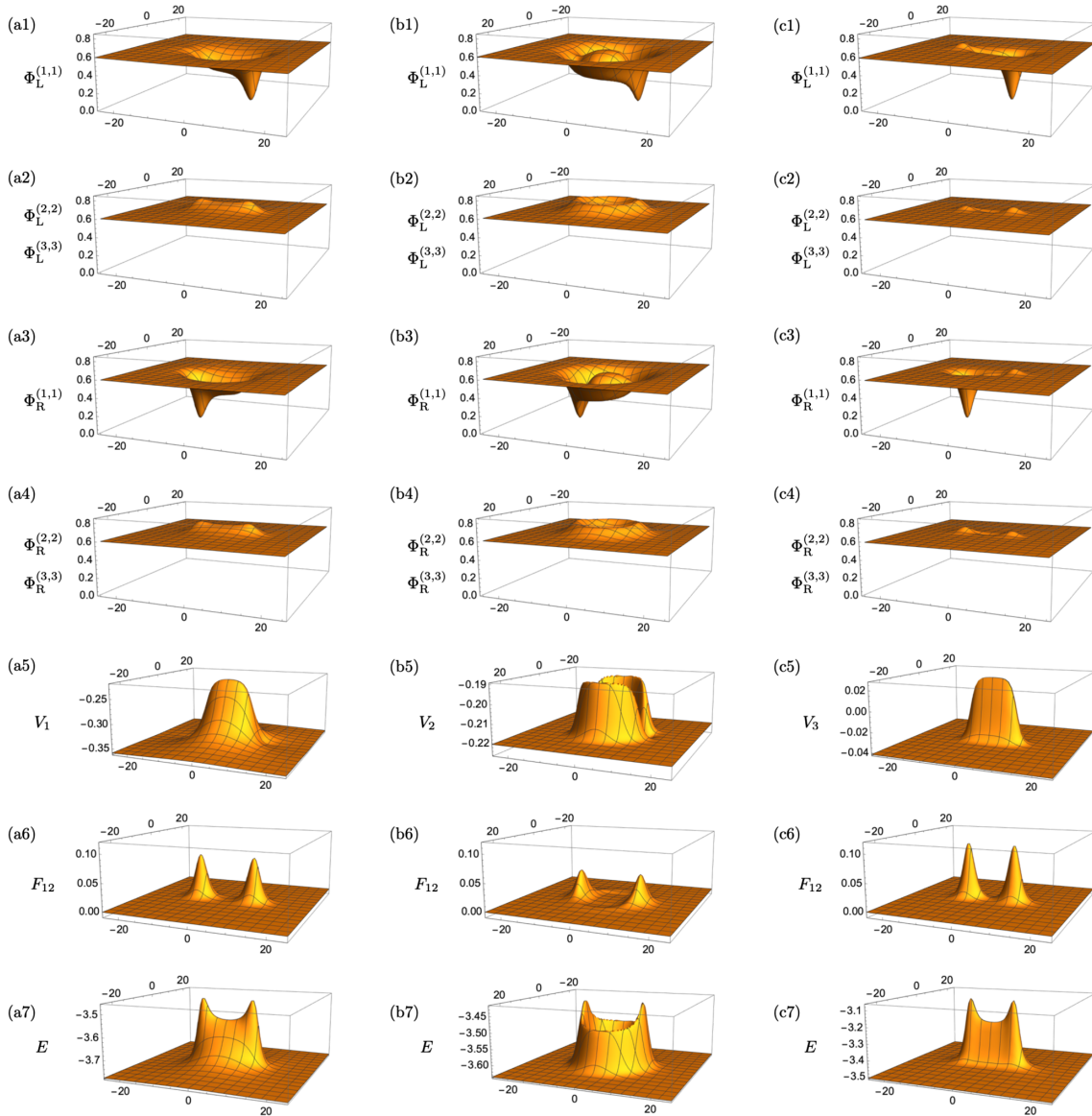


FIG. 4. The profile functions  $|\Phi_{L,R}^{(i,i)}|^2$  ( $i = 1, 2, 3$ ) of a pair of the  $(1, 0)$  and  $(0, 1)$  chiral non-Abelian vortices. They are stretched by a chiral domain wall(s). The parameter choice of the left-most, middle, and right-most columns are  $(\gamma_1, \gamma_2, \gamma_3) = (0.01, 0, 0)$ ,  $(0, 0.01, 0)$ ,  $(0, 0, 0.2)$ , respectively. The other parameters are common for all cases as  $(m, \lambda_1, \lambda_2, \lambda_3, \lambda_4, g) = (\sqrt{2}, 1, 1, 1, 0, 1)$ .

is no wall along the path  $b_1 + b_2$  encircling the whole configuration. Dynamically, the domain wall tension pulls these chiral non-Abelian vortices and combine them to a single non-Abelian semisuperfluid vortex. Thus, these chiral non-Abelian vortices are confined to a “mesonic” configuration, which is nothing but a non-Abelian semisuperfluid vortex. We can express this confining process by

$$(1, 0) + (0, 1) \rightarrow (1, 1). \quad (8.5)$$

In Fig. 4, we present numerical simulations of a pair of chiral non-Abelian vortices  $(1, 0)$  and  $(0, 1)$  separated at finite distance. Clearly one can see that the domain walls are stretched between them. In the case of  $(\gamma_1, \gamma_2, \gamma_3) = (*, 0, 0)$  (the left column), a single non-Abelian

sine-Gordon kink is stretched between them. In the case of  $(\gamma_1, \gamma_2, \gamma_3) = (0, *, 0)$  (the middle column), two domain walls are stretched between them forming a ring, like vortex molecules in a chiral P-wave superconductor, see footnote 7.1. Finally, in the case of  $(\gamma_1, \gamma_2, \gamma_3) = (0, 0, *)$  (the right column), a single Abelian sine-Gordon kink is stretched between them.

The two vortices are linearly confined and these configurations are on a way to collapse. It is an open question whether, as the case of two-component BECs ( $N = 1$ ), these constituents can be separated at finite distance and an internal structure of the molecule is visible in certain parameter regions. Possibly, it may occur when  $\lambda_4 (> 0)$  is large enough for which the  $(1, 0)$  and  $(0, 1)$  vortices

would repel each other at short distances. Explicitly constructing numerical solutions remains a future problem.

### B. Generalized Aharonov-Bohm phases

Let us discuss generalized AB phases around a vortex molecule in Fig. 3(b). We restrict to  $N = 3$  relevant for the CFL phase.

When the light quarks encircle the  $(1, 0)$ -vortex at L along the path  $b_L - r$ , they receive the generalized AB phases

$$\begin{aligned} q_L &\rightarrow \left( \begin{array}{c|c} -(q_L)_{11} & (q_L)_{1j} \\ \hline (q_L)_{i1} & -(q_L)_{ij} \end{array} \right), \\ q_R &\rightarrow \left( \begin{array}{c|c} (q_R)_{11} & -(q_R)_{1j} \\ \hline -(q_R)_{i1} & (q_R)_{ij} \end{array} \right). \end{aligned} \quad (8.6)$$

These constitute a  $\mathbb{Z}_2$  group, which is a color nonsinglet. On the other hand, when they encircle the  $(0, 1)$ -vortex at R along the path  $b_R + r$ , they receive the generalized AB phases

$$\begin{aligned} q_L &\rightarrow \left( \begin{array}{c|c} (q_L)_{11} & -(q_L)_{1j} \\ \hline -(q_L)_{i1} & (q_L)_{ij} \end{array} \right), \\ q_R &\rightarrow \left( \begin{array}{c|c} -(q_R)_{11} & (q_R)_{1j} \\ \hline (q_R)_{i1} & -(q_R)_{ij} \end{array} \right), \end{aligned} \quad (8.7)$$

constituting a  $\mathbb{Z}_2$  group, which is a color nonsinglet.

Thus, when they encircle the both vortices along the large circle  $b_L + b_R$ , they receive the generalized AB phases

$$q_L \rightarrow -q_L, \quad q_R \rightarrow -q_R, \quad (8.8)$$

constituting a  $\mathbb{Z}_2$  group. This is a color singlet. These generalized AB phases are precisely those of a single non-Abelian semisuperfluid vortex [31,32]. Interestingly, the light quarks can detect the color of fluxes of the chiral non-Abelian vortices  $(1, 0)$  and  $(0, 1)$  at the large distance by the generalized AB phases in Eqs. (8.6) and (8.7) which are color nonsinglets, but they cannot detect the color of the flux of the whole molecule by the generalized AB phase in Eq. (8.8) which is a color singlet.

As for heavy quarks, they detect only gauge fields. Thus, they do not distinguish the  $(1, 0)$ - and  $(0, 1)$ -vortices unlike the light quarks, since the gauge structures are identical between these two vortices carrying exactly the same color magnetic fluxes. Therefore, when they encircle either of the  $(1, 0)$ - and  $(0, 1)$ -vortices, they receive the AB phases in Eq. (5.20) which is a color nonsinglet, while when they encircle the both of them along the path  $b_L + b_R$ , they receive the AB phases in Eq. (5.22) which is a color singlet.

The latter forming a color singlet  $\mathbb{Z}_3$  group are precisely those of a single non-Abelian vortex [37].

In summary, chiral non-Abelian vortices are not confined and can exist alone when  $\gamma_{1,2,3} = 0$ , while they are confined when  $\gamma_{1,2,3} \neq 0$ . In the deconfined phase, chiral non-Abelian vortices exhibit color nonsinglet (generalized) AB phases so that the light/heavy quarks can detect the colors of magnetic fluxes of these vortices at large distances. In the confined phase, chiral non-Abelian vortices exhibit only color singlet (generalized) AB phases so that the light/heavy quarks cannot detect the colors of magnetic fluxes of these vortices at large distances. Thus, stable states exhibit color-singlet (generalized) AB phases.

The opposite is not always true. Not all states with color-singlet (generalized) AB phases can exist stably in the confined phase. For instance, the two examples  $(1, -1)$  and  $(2, 0)$  in Sec. VII B exhibit color-singlet (generalized) AB phases; the  $(2, 0)$  made of two  $(1, 0)$  with the same color magnetic fluxes exhibits the singlet AB phase for heavy quarks in Eq. (5.22) and the trivial phases for light quarks obtained from two successive phases of Eq. (5.24);  $(Q_L, Q_R, q_L, q_R) \rightarrow (\epsilon^2 Q_L, \epsilon^2 Q_R, q_L, q_R)$ , which are color singlet. Nevertheless, they are attached by the two chiral domain walls extending to infinities as in Fig. 3(a), and are unstable against decay into two chiral non-Abelian vortices each of which is attached by one (or two) chiral domain wall(s):  $(1, -1) \rightarrow (1, 0) + (0, -1)$  and  $(2, 0) \rightarrow 2(1, 0)$ . The  $(N, 0)$  vortex made of  $N$   $(1, 0)$  vortices with all different color magnetic fluxes give generalized AB phases as  $(Q_L, Q_R, q_L, q_R) \rightarrow (Q_L, Q_R, -q_L, q_R)$ , which are color singlets. It is, however, broken as  $(N, 0) \rightarrow N(1, 0)$ .

## IX. SUMMARY AND DISCUSSION

In the CFL phase of dense QCD, we have found chiral non-Abelian vortices winding only around either of left or right diquark condensation  $\Phi_L$  or  $\Phi_R$  labeled by  $(1, 0)$  and  $(0, 1)$ , respectively. As can be expected from  $(1, 0) = \frac{1}{2}[(1, 1) + (1, -1)]$  and  $(0, 1) = \frac{1}{2}[(1, 1) - (1, -1)]$ , they carry half color magnetic fluxes and half  $U(1)_B$  circulation of those of a non-Abelian semisuperfluid vortex labeled by  $(1, 1)$ , and half  $U(1)_A$  winding and half chiral circulation [around the sub-OPM  $\mathcal{M}_A = U(N)_{L-R+A}$ ] of a non-Abelian axial vortex labeled by  $(1, -1)$ . A single chiral non-Abelian vortex carries  $\mathbb{C}P^{N-1}$  orientational moduli in the internal space corresponding to its color magnetic flux. We have discussed the energetics of vortices and have found that  $\mathbb{C}P^{N-1}$  orientations of two chiral non-Abelian vortices  $(1, 0)$  and  $(0, 1)$  are energetically aligned, while those with a chiral vortex  $(1, 0)$  and antivortex  $(0, -1)$  are energetically orthogonal to each other. Then, the two chiral non-Abelian vortices attract each other forming bound states. We have shown that chiral non-Abelian vortices exhibit the topological obstruction implying that the unbroken symmetry generators are not defined globally

around the vortices, and color nonsinglet (generalized) AB phases implying that quarks at large distances can detect the colors of magnetic fluxes by encircling these vortices. In the presence of the axial and chiral symmetry breaking terms  $\gamma_{1,2,3} \neq 0$ , these vortices are confined by chiral domain walls, while they are deconfined in the absence of those terms. In the confined phase, two chiral non-Abelian vortices  $(1, 0)$  and  $(0, 1)$  with chiralities opposite to each other are connected by a chiral domain wall, constituting a mesonic bound state  $(1, 1)$  which is nothing but a non-Abelian semisuperfluid vortex, exhibiting only color singlet (generalized) AB phases implying that the quarks cannot detect the color of magnetic flux of such a bound state at large distances. We also have shown that the Abelian axial vortices  $(N, -N)$  and non-Abelian axial vortices  $(1, -1)$  attached by chiral domain walls are both unstable to decay into a set of chiral non-Abelian vortices.

Before closing this paper, let us address several discussions and future directions.

The confinement does not imply that the mesonic bound state necessary collapses to an axisymmetric non-Abelian semisuperfluid vortex. It remains as a future problem to numerically construct solutions of vortex molecules in certain parameter regions, in which the constituent  $(1, 0)$  and  $(0, 1)$  vortices are separated at finite distances. At least the axial and chiral symmetry breaking terms should be relatively small. At finite temperature, it does not have to be the case at least in  $2 + 1$  dimensions because of the Berezinskii-Kosterlitz-Thouless (BKT) transition. The BKT transition was explicitly shown in Ref. [53] by numerical simulations for the Abelian case  $N = 1$ .

In this paper, we have constructed numerical solutions for single chiral non-Abelian vortices  $(1, 0)$  or  $(0, 1)$ , in the absence of the axial and chiral symmetry breaking terms:  $\gamma_{1,2,3} = 0$ . In the presence of these terms, chiral domain walls are attached to them. We have constructed solutions in the case that only one of  $\gamma_{1,2,3}$  is nonzero. In particular, if we turn on all  $\gamma_{1,2,3}$ 's, the situation is close to the two-Higgs doublet models [24,25]. Explicitly constructing numerical solutions of such domain-wall vortex composites in general cases remains as one of future problems. A particularly important problem is to construct a vortex molecule  $(1, 0) + (0, 1)$ . This would reduce to a single non-Abelian semisuperfluid vortex in the most parameter region because of the domain wall tension, but we should examine whether these two constituents can be separated in some parameter region particularly for small  $\gamma_{1,2,3}$ 's and/or small gauge coupling  $g_s$  for which there is a repulsion between constituent vortices. This problem is important in a relation with higher-form symmetries discussed in the next paragraph. Finally, we also should numerically verify decays of axial and chiral vortices as discussed in Sec. VII B, such as a non-Abelian axial vortex  $(1, -1) \rightarrow (1, 0) + (0, -1)$  and an Abelian axial vortex  $(N, -N) \rightarrow N(1, 0) + N(0, 1)$ , as we did a similar problem in the linear sigma models [5,54].

In particular, in the presence of the mass terms  $\gamma_{1,2} \neq 0$ ,  $2N$  domain walls attached to one Abelian axial vortex  $(N, -N)$  constitute a composite wall as can be expected from Eq. (4.2), and it is an open question whether this fact suppresses the decay. To perform simulations, we may do either a relaxation method or real time dynamics. For the latter, we need a time-dependent GL theory.

Higher-form symmetries [84] related with a linking between Wilson loops and vortices are an indispensable tool to study phases of matter such as the so-called topological order. Higher form symmetries in the presence of non-Abelian semisuperfluid vortices and the absence or presence of a topological order of the CFL phase were studied in Refs. [39–42,85]. In this case, a linking between a Wilson loop and a non-Abelian semisuperfluid vortex is rather trivial in the sense that AB phases are color singlets. Contrary to this, a linking between a Wilson loop and a chiral non-Abelian vortex is nontrivial because AB phases are color nonsinglets as we have seen in Sec. V C. Thus, the phase separating a non-Abelian semisuperfluid vortex  $(1, 1)$  into two chiral non-Abelian vortices  $(1, 0)$  and  $(0, 1)$  may be characterized in terms of a higher-form symmetry.

As mentioned in introduction, in the context of quark-hadron continuity, vortices penetrate through the CFL phase and hyperon nuclear matter [9,36–42]. In particular, from the AB phases of quarks around vortices, one can conclude the existence of a boojum at which three hyperon vortices and three non-Abelian semisuperfluid vortices must meet [9,37,38]. This structure is modified if the deconfined phase is realized in the CFL phase. In fact, this situation is similar to two-flavor quark matter (see Appendix C).

Beyond the GL description, we could study fermion structure by the BdG formulation. In fact, fermion zero modes were studied for non-Abelian semisuperfluid vortices in the BdG equation [31–33], in which triplet Majorana fermion zero modes were found. Such Majorana fermions endow these vortices non-Abelian exchange statistics in  $d = 2 + 1$ , turning them into non-Abelian anyons [86,87]. Apparently, it is a very interesting question whether fermion zero modes exist on chiral non-Abelian vortices and if so what their exchange statistics are.

The  $\mathbb{C}P^2$  modes of the chiral non-Abelian vortex are probably non-normalizable, unlike those of a single non-Abelian semisuperfluid vortex [5,30]. However, around a constituent of a vortex molecule  $(1, 1)$ , these modes may be normalizable because of a cutoff introduced by the presence of the other. The  $\mathbb{C}P^2$  modes are normalizable on the chiral domain wall [82,83] that connects the  $(1, 0)$  and  $(0, 1)$ . This fact together with the fact that the  $\mathbb{C}P^2$  modes are normalizable on a single non-Abelian semisuperfluid vortex [5,30] may suggest that these modes are still normalizable around the vortex molecule  $(1, 1)$ .

In this paper, we have turned off the electro-magnetic interaction and the strange quark mass. Turning them on

can be incorporated in the  $\mathbb{C}P^2$  effective world-sheet Lagrangian of a single non-Abelian semisuperfluid vortex in Refs. [88,30], respectively. This method may be applied to the case of a chiral non-Abelian vortex as well.

Finally, there are some interesting directions for studying chiral domain walls. One is a decay of chiral domain walls by quantum or thermal tunneling. In this case, a hole created on the domain wall world volume is surrounded by an axial vortex (see Sec. 10.5 of the review paper [5]). For the minimum element of a chiral domain wall, a hole should be surrounded by a chiral non-Abelian vortex studied in this paper. The other direction is given by the chiral non-Abelian semisuperfluid vortices under magnetic field background which would be also interesting in connection with the chiral anomaly. The domain wall connecting (1, 0) and (0, 1) is made of the  $\eta'$  meson related to  $U(1)_A$ , and  $\eta'$  nontrivially changes along the direction perpendicular to the  $\eta'$  domain wall. Therefore, under the presence of magnetic field, the domain wall should be magnetized as found in Refs. [89,90], see also Sec. 10.6 of Ref. [5]. Physical consequences of these domain walls are interesting to explore.

## ACKNOWLEDGMENTS

The work of M. E. is supported in part by JSPS Grant-in-Aid for Scientific Research KAKENHI Grant No. JP19K03839, and by MEXT KAKENHI Grant-in-Aid for Scientific Research on Innovative Areas ‘‘Discrete Geometric Analysis for Materials Design’’ No. JP17H06462 from the MEXT of Japan. The work of M. N. is supported in part by JSPS KAKENHI Grant No. 18H01217.

## APPENDIX A: TERMINOLOGIES

In this Appendix, we summarize terminologies in this paper, which may be sometimes confusing.

### 1. Abelian and Non-Abelian

The terminology ‘‘Abelian vortices’’ is used for vortices having winding in a  $U(1)$  group. In this paper, such a  $U(1)$  group is either the baryonic symmetry  $U(1)_B$  or axial symmetry  $U(1)_A$ . A vortex winding around  $U(1)_B$  is called an Abelian superfluid vortex (Sec. III A), while one winding around  $U(1)_A$  is called an axial vortex (Sec. IV A).

In this paper, the terminology ‘‘non-Abelian’’ is used for vortices with non-Abelian magnetic fluxes and those accompanied with non-Abelian Nambu-Goldstone modes, as is common in dense QCD [5,11], supersymmetric QCD [14–19] (see Refs. [20–23] as a review), and two-Higgs doublet models [24–28].

Global analogues are also called non-Abelian. In this paper, vortices winding in chiral symmetry breaking  $U(N)_L \times U(N)_R \rightarrow SU(N)_{L+R}$  are called non-Abelian axial vortices, see Sec. IV B.

However note that the same terminology ‘‘non-Abelian’’ is sometimes used for a different meaning in the literature. It is used for vortices with non-Abelian holonomies in Refs. [56–58], which differs from our terminology. Note that the above mentioned non-Abelian vortices in dense QCD, SUSY QCD and two-Higgs doublet models are *Abelian* in this language since holonomies are  $\mathbb{Z}_N$  ( $N = 3$  for dense QCD and  $N = 2$  for two-Higgs doublet models). Chiral non-Abelian vortices found in this paper are accompanied by non-Abelian holonomies, and thus they are non-Abelian in this language as well.

### 2. Superfluid/semisuperfluid

Abelian superfluid vortices have integer windings around  $U(1)_B$ . They do not carry any color magnetic fluxes.

Semisuperfluid vortices have fractional windings around  $U(1)_B$ . For single-valuedness, they must be accompanied with color gauge transformation for single-valuedness of fields, and thus they are inevitably non-Abelian.

### 3. Chiral

We call vortices ‘‘chiral’’ when only  $\Phi_L$  or  $\Phi_R$  has windings. We label it by (1, 0) or (0, 1).

### 4. Topological obstruction

Here, we explain the topological obstruction [55–62]. When a symmetry  $G$  is spontaneously broken down to its subgroup  $H$ , the OPM is a coset space  $G/H$ . Note that the unbroken symmetry  $H$  is not unique. When the VEV  $v = \langle \phi \rangle$  of a field  $\phi$  is transformed to  $v' = gv$  with some group element  $g \in G$ , the unbroken symmetry  $H$  is also transformed to  $H' = gHg^{-1}$ .

A problem may happen in the presence of a vortex. When we put a vortex, the asymptotic value of the field  $\phi$  depends on the azimuthal angle  $\varphi$  around the vortex:  $\phi(\varphi) \sim g(\varphi)v$ . Around the vortex, the unbroken symmetry  $H$  depends on the azimuthal angle  $\varphi$  as  $H_\varphi = g(\varphi)H_0g(\varphi)^{-1}$  with  $H_0$  being  $H$  at  $\varphi = 0$ . From the single-valuedness of  $\phi$ , we have  $\phi(\varphi = 2\pi) = \phi(\varphi = 0)$ . However, this does not necessarily imply  $g(\varphi = 2\pi) = g(\varphi = 0)$ . In general,  $g(\varphi = 2\pi) \neq g(\varphi = 0)$ , and thus the unbroken symmetry is not single-valued:  $H_{\varphi=2\pi} \neq H_{\varphi=0} = H_0$ . This is the topological obstruction. An example can be found in an Alice string [55].

## APPENDIX B: ORDER PARAMETER MANIFOLDS

Let us describe the full OPM in this Appendix. To this end, we neglect explicit breaking terms,  $\gamma_{1,2,3} = 0$ , thus axial and chiral symmetries becoming exact.

The symmetry  $G$  acts on the condensates  $\Phi_{L,R}$ , which are  $N$  by  $N$  matrices of complex scalar fields, as

TABLE II. Summary table of the discrete symmetries.  $\omega$  is the  $N$ -th root of the unity:  $\omega = \exp(2\pi i/N)$ . Note  $(\mathbb{Z}_N)_{C+L+r} = (\mathbb{Z}_N)_{C+B}$ .

	$SU(N)_C$	$SU(N)_L$	$SU(N)_R$	$U(1)_l$	$U(1)_r$	$U(1)_B$	$U(1)_A$
$(\mathbb{Z}_N)_C$	$\omega^k$	1	1	1	1	1	1
$(\mathbb{Z}_N)_L$	1	$\omega^k$	1	1	1	1	1
$(\mathbb{Z}_N)_R$	1	1	$\omega^k$	1	1	1	1
$(\mathbb{Z}_N)_l$	1	1	1	$\omega^k$	1	$\omega^{-\frac{k}{2}}$	$\omega^{-\frac{k}{2}}$
$(\mathbb{Z}_N)_r$	1	1	1	1	$\omega^k$	$\omega^{-\frac{k}{2}}$	$\omega^{\frac{k}{2}}$
$(\mathbb{Z}_N)_B$	1	1	1	$\omega^{-k}$	$\omega^{-k}$	$\omega^k$	1
$(\mathbb{Z}_N)_A$	1	1	1	$\omega^{-k}$	$\omega^k$	1	$\omega^k$
$(\mathbb{Z}_N)_{C+L+r}$	$\omega^k$	1	1	$\omega^k$	$\omega^k$	$\omega^{-k}$	1
$(\mathbb{Z}_N)_{L+l}$	1	$\omega^k$	1	$\omega^{-k}$	1	$\omega^{\frac{k}{2}}$	$\omega^{\frac{k}{2}}$
$(\mathbb{Z}_N)_{R+r}$	1	1	$\omega^k$	1	$\omega^{-k}$	$\omega^{\frac{k}{2}}$	$\omega^{-\frac{k}{2}}$
$(\mathbb{Z}_N)_{C+B}$	$\omega^k$	1	1	$\omega^k$	$\omega^k$	$\omega^{-k}$	1
$(\mathbb{Z}_N)_{L+R+B}$	1	$\omega^k$	$\omega^k$	$\omega^{-k}$	$\omega^{-k}$	$\omega^k$	1
$(\mathbb{Z}_N)_{L-R+A}$	1	$\omega^k$	$\omega^{-k}$	$\omega^{-k}$	$\omega^k$	1	$\omega^k$
$(\mathbb{Z}_N)_{C+L+R}$	$\omega^k$	$\omega^k$	$\omega^k$	1	1	1	1
$(\mathbb{Z}_N)_{C-(L+R)+B}$	$\omega^k$	$\omega^{-k}$	$\omega^{-k}$	$\omega^{2k}$	$\omega^{2k}$	$\omega^{-2k}$	1
$(\mathbb{Z}_2)_{A+B}$	1	1	1	1	1	-1	-1

$$\begin{aligned} \Phi_L &\rightarrow g_C \Phi_L \hat{U}_L^\dagger, & \Phi_R &\rightarrow g_C \Phi_R \hat{U}_R^\dagger \\ g_C &\in SU(N)_C, & \hat{U}_{L,R} &\in U(N)_{L,R}. \end{aligned} \quad (\text{B1})$$

With taking into account discrete groups,  $G$  can be faithfully written as

$$\begin{aligned} G &= \frac{SU(N)_C \times U(N)_L \times U(N)_R}{(\mathbb{Z}_N)_{C+L+r}} \\ &= \frac{SU(N)_C \times U(1)_l \times U(1)_r \times SU(N)_L \times SU(N)_R}{(\mathbb{Z}_N)_{C+L+r} \times (\mathbb{Z}_N)_{L+l} \times (\mathbb{Z}_N)_{R+r}} \end{aligned} \quad (\text{B2})$$

with

$$\begin{aligned} U(N)_L &= \frac{U(1)_l \times SU(N)_L}{(\mathbb{Z}_N)_{L+l}}, \\ U(N)_R &= \frac{U(1)_r \times SU(N)_R}{(\mathbb{Z}_N)_{R+r}}. \end{aligned} \quad (\text{B3})$$

Here, the discrete groups  $\mathbb{Z}_N$  are defined in Table II, and the two  $U(1)$  groups can be explicitly written as

$$\begin{aligned} U(1)_l: & (\Phi_L, \Phi_R) \rightarrow (e^{-i\theta_l} \Phi_L, \Phi_R), \\ U(1)_r: & (\Phi_L, \Phi_R) \rightarrow (\Phi_L, e^{-i\theta_r} \Phi_R). \end{aligned} \quad (\text{B4})$$

Let us rewrite the two  $U(1)$  groups in Eq. (B4) by the baryon and axial  $U(1)$  groups as

$$\begin{aligned} U(1)_B: & (\Phi_L, \Phi_R) \rightarrow e^{i\theta_B} (\Phi_L, \Phi_R), \\ U(1)_A: & (\Phi_L, \Phi_R) \rightarrow (e^{i\theta_A} \Phi_L, e^{-i\theta_A} \Phi_R), \end{aligned} \quad (\text{B5})$$

where the relation is given by

$$\theta_B = -\frac{\theta_l + \theta_r}{2}, \quad \theta_A = -\frac{\theta_l - \theta_r}{2}. \quad (\text{B6})$$

Note that

$$U(1)_l \times U(1)_r = \frac{U(1)_B \times U(1)_A}{(\mathbb{Z}_2)_{A+B}}, \quad (\text{B7})$$

where  $(\mathbb{Z}_2)_{A+B}$  generated by  $(-1, -1) \in U(1)_B \times U(1)_A$  is redundant and must be removed. Then, the symmetry  $G$  acting on the condensates as

$$\begin{aligned} \Phi_L &\rightarrow e^{i\theta_B + i\theta_A} g_C \Phi_L U_L^\dagger, & \Phi_R &\rightarrow e^{i\theta_B - i\theta_A} g_C \Phi_R U_R^\dagger \\ g_C &\in SU(N)_C, & U_{L,R} &\in SU(N)_{L,R}, & e^{i\theta_B} &\in U(1)_B, \\ e^{i\theta_A} &\in U(1)_A \end{aligned} \quad (\text{B8})$$

can be rewritten as

$$G = \frac{SU(N)_C \times U(1)_B \times U(1)_A \times SU(N)_L \times SU(N)_R}{(\mathbb{Z}_2)_{A+B} \times (\mathbb{Z}_N)_{C+B} \times (\mathbb{Z}_N)_{L+R+B} \times (\mathbb{Z}_N)_{L-R+A}} \\ = \frac{SU(N)_C \times U(1)_B \times U(1)_A \times SU(N)_L \times SU(N)_R}{(\mathbb{Z}_2)_{A+B} \times (\mathbb{Z}_N)_{C+L+R} \times (\mathbb{Z}_N)_{C-(L+R)+B} \times (\mathbb{Z}_N)_{L-R+A}}, \quad (\text{B9})$$

with the discrete groups in the denominator, defined in Table II. In Eq. (B9), the direct product of the two groups have been rewritten by taking the product of the former groups as  $(\mathbb{Z}_N)_{C+B} \times (\mathbb{Z}_N)_{L+R+B} = (\mathbb{Z}_N)_{C+L+R} \times (\mathbb{Z}_N)_{C-(L+R)+B}$  for later convenience.

The unbroken subgroup  $H$  on the ground state  $\Phi_L \sim \Phi_R \sim v\mathbf{1}_N$  is

$$H = \frac{SU(N)_{C+L+R} \times (\mathbb{Z}_N)_{C-(L+R)+B} \times (\mathbb{Z}_N)_{L-R+A}}{(\mathbb{Z}_N)_{C+L+R} \times (\mathbb{Z}_N)_{C-(L+R)+B} \times (\mathbb{Z}_N)_{L-R+A}} = \frac{SU(N)_{C+L+R}}{(\mathbb{Z}_N)_{C+L+R}}, \quad (\text{B10})$$

where the same rearrangements of the discrete groups with Eq. (B2) have been taken in the denominator.

Thus, the full OPM can be obtained as

$$\mathcal{M} = \frac{G}{H} = \frac{SU(N)_C \times U(1)_B \times U(1)_A \times SU(N)_L \times SU(N)_R}{SU(N)_{C+L+R} \times (\mathbb{Z}_N)_{C-(L+R)+B} \times (\mathbb{Z}_N)_{L-R+A} \times (\mathbb{Z}_2)_{A+B}}. \quad (\text{B11})$$

Note the relation

$$SU(N)_L \times SU(N)_R = SU(N)_{L+R} \ltimes \frac{SU(N)_L \times SU(N)_R}{SU(N)_{L+R}} \\ \simeq SU(N)_{L+R} \ltimes SU(N)_{L-R}, \quad (\text{B12})$$

where  $F \ltimes B$  denotes a fiber bundle with a fiber  $F$  over a base manifold  $B$ .<sup>6</sup> We can further rewrite it as

$$\mathcal{M} = \left[ \frac{U(1)_B \times SU(N)_{C-(L+R)}}{(\mathbb{Z}_N)_{C-(L+R)+B}} \ltimes \frac{U(1)_A \times SU(N)_{L-R}}{(\mathbb{Z}_N)_{L-R+A}} \right] / (\mathbb{Z}_2)_{A+B} \\ = \frac{U(N)_{C-(L+R)+B} \ltimes U(N)_{L-R+A}}{(\mathbb{Z}_2)_{A+B}} = \frac{\mathcal{M}_V \ltimes \mathcal{M}_A}{(\mathbb{Z}_2)_{A+B}}. \quad (\text{B13})$$

Here, we have defined the OPMs for the vector symmetry breaking and for the axial and chiral symmetry breakings by

$$\mathcal{M}_V \simeq \frac{U(1)_B \times SU(N)_C \times SU(N)_{L+R}}{(\mathbb{Z}_N)_{C-(L+R)+B} \times SU(N)_{C+L+R}} \simeq \frac{U(1)_B \times SU(N)_{C-(L+R)}}{(\mathbb{Z}_N)_{C-(L+R)+B}} \simeq U(N)_{C-(L+R)+B}, \\ \mathcal{M}_A \simeq \frac{U(1)_A \times SU(N)_L \times SU(N)_R}{(\mathbb{Z}_N)_{L-R+A} \times SU(N)_{L+R}} \simeq \frac{U(1)_A \times SU(N)_{L-R}}{(\mathbb{Z}_N)_{L-R+A}} \simeq U(N)_{L-R+A}, \quad (\text{B14})$$

with coset spaces

$$SU(N)_{C-(L+R)} \simeq \frac{SU(N)_C \times SU(N)_{L+R}}{SU(N)_{C+L+R}}, \quad SU(N)_{L-R} \simeq \frac{SU(N)_L \times SU(N)_R}{SU(N)_{L+R}}. \quad (\text{B15})$$

<sup>6</sup>In general, when a Lie group  $G$  is spontaneously broken down to  $H$ , the OPS parametrized by Nambu-Goldstone modes is a coset space  $G/H$ . In this situation, the original group  $G$  can be regarded as a (principal) fiber bundle  $H \ltimes B$  over the base space  $B \simeq G/H$  with a fiber  $H$ . In our case,  $H = SU(N)_{L+R}$  and  $G/H = \frac{SU(N)_L \times SU(N)_R}{SU(N)_{L+R}} \simeq SU(N)_{L-R}$ . Here, note that  $G/H$  is not endowed with a product but isomorphic to a Lie group that we denote by  $SU(N)_{L-R}$ .

### APPENDIX C: SIMILARITIES AND DIFFERENCES WITH VORTICES IN TWO-FLAVOR DENSE QCD

Let us make comments on possible similarities with recently found non-Abelian Alice strings in two-flavor dense QCD.

Recently, two-flavor dense QCD relevant for quark-hadron continuity was proposed [71,72], consisting of the 2SC condensation of up and down quarks in addition to a P-wave condensation of down quarks. This phase is referred as the  $2SC + \langle dd \rangle$  phase and is further classified into deconfined and confined phases of vortices. In the deconfined phase, the most stable vortices are non-Abelian Alice strings which are superfluid vortices carrying color magnetic fluxes [68–70]. The amount of these color magnetic fluxes are half of those of non-Abelian semisuperfluid vortices in the CFL phase.

These are non-Abelian analogue of Alice strings [55–61], and in particular are an  $SU(3) \times U(1)$  extension of Alice strings in  $SU(2) \times U(1)$  gauge theory [91–94].

One of the characteristic features of non-Abelian Alice strings is that unbroken symmetry generators are not globally defined around the strings, and in general they are multivalued (topological obstruction). Another characteristic feature, which is more important, is that particles encircling these strings can detect the colors of the strings from infinite distances by color nonsinglet AB phases.

In the confined phase, non-Abelian Alice strings are confined by the so-called AB defects [93–95] appearing to compensate a discontinuity originated from nontrivial AB phases of the 2SC condensation [70]. As a result of vortex confinement, there can exist only baryonic and mesonic

bound states of the Alice strings, which exhibit color singlet AB phases of particles encircling them; The baryonic bound state consists of three Alice strings with different (red, blue, green) color magnetic fluxes with total color canceled out, which are connected by a domain wall junction resulting in a single Abelian superfluid vortex, while the mesonic bound state consists of two Alice strings with the same color magnetic fluxes, which are connected by a single domain wall resulting in a doubly-wound non-Abelian string. Although the latter carries a color magnetic flux, it can exist because of color-singlet AB phases, that is, the color cannot be detected from infinite distance by AB phases of particles encircling it. The amount of the color magnetic flux that the mesonic bound state of the Alice string (or doubly-wound non-Abelian vortex) in two-flavor quark matter is the same with that of a non-Abelian string in the CFL phase.

Moreover, both of a mesonic bound state of the Alice string (or doubly-wound non-Abelian vortex) in two-flavor quark matter and a non-Abelian string in the CFL phase exhibit  $\mathbb{Z}_3$  color-singlet AB phases of heavy quarks, and  $\mathbb{Z}_2$  color-singlet generalized AB phases of light quarks. However, a crucial difference between them is that non-Abelian Alice strings are confined by the AB defects *spontaneously* appearing in the formation of the 2SC condensate while chiral non-Abelian vortices are confined by chiral domain walls existing due to the *explicit breaking* (mass and anomaly terms) of the axial and chiral symmetries. Thus, we can summarize that a salient distinction is whether the appearance of the domain walls confining the vortices is due to spontaneous (the  $2SC + \langle dd \rangle$  phase) or explicit (the CFL phase) breaking.

- 
- [1] M. G. Alford, A. Schmitt, K. Rajagopal, and T. Schäfer, *Rev. Mod. Phys.* **80**, 1455 (2008).
  - [2] M. G. Alford, K. Rajagopal, and F. Wilczek, *Nucl. Phys.* **B537**, 443 (1999).
  - [3] M. G. Alford, K. Rajagopal, and F. Wilczek, *Phys. Lett. B* **422**, 247 (1998).
  - [4] R. Rapp, T. Schäfer, E. V. Shuryak, and M. Velkovsky, *Phys. Rev. Lett.* **81**, 53 (1998).
  - [5] M. Eto, Y. Hirono, M. Nitta, and S. Yasui, *Prog. Theor. Exp. Phys.* **2014**, 012D01 (2014).
  - [6] M. M. Forbes and A. R. Zhitnitsky, *Phys. Rev. D* **65**, 085009 (2002).
  - [7] K. Iida and G. Baym, *Phys. Rev. D* **66**, 014015 (2002).
  - [8] E. Nakano, M. Nitta, and T. Matsuura, *Phys. Rev. D* **78**, 045002 (2008).
  - [9] M. Cipriani, W. Vinci, and M. Nitta, *Phys. Rev. D* **86**, 121704 (2012).
  - [10] M. G. Alford, S. Mallavarapu, T. Vachaspati, and A. Windisch, *Phys. Rev. C* **93**, 045801 (2016).
  - [11] A. Balachandran, S. Dikal, and T. Matsuura, *Phys. Rev. D* **73**, 074009 (2006).
  - [12] E. Nakano, M. Nitta, and T. Matsuura, *Prog. Theor. Phys. Suppl.* **174**, 254 (2008).
  - [13] M. Eto and M. Nitta, *Phys. Rev. D* **80**, 125007 (2009).
  - [14] A. Hanany and D. Tong, *J. High Energy Phys.* **07** (2003) 037.
  - [15] R. Auzzi, S. Bolognesi, J. Evslin, K. Konishi, and A. Yung, *Nucl. Phys.* **B673**, 187 (2003).
  - [16] A. Hanany and D. Tong, *J. High Energy Phys.* **04** (2004) 066.
  - [17] M. Shifman and A. Yung, *Phys. Rev. D* **70**, 045004 (2004).
  - [18] M. Eto, Y. Isozumi, M. Nitta, K. Ohashi, and N. Sakai, *Phys. Rev. D* **72**, 025011 (2005).
  - [19] M. Eto, Y. Isozumi, M. Nitta, K. Ohashi, and N. Sakai, *Phys. Rev. Lett.* **96**, 161601 (2006).
  - [20] D. Tong, arXiv:hep-th/0509216.
  - [21] M. Eto, Y. Isozumi, M. Nitta, K. Ohashi, and N. Sakai, *J. Phys. A* **39**, R315 (2006).
  - [22] M. Shifman and A. Yung, *Rev. Mod. Phys.* **79**, 1139 (2007).

- [23] M. Shifman and A. Yung, *Supersymmetric Aolitions*, Cambridge Monographs on Mathematical Physics (Cambridge University Press, Cambridge, England, 2009).
- [24] M. Eto, M. Kurachi, and M. Nitta, *Phys. Lett. B* **785**, 447 (2018).
- [25] M. Eto, M. Kurachi, and M. Nitta, *J. High Energy Phys.* **08** (2018) 195.
- [26] M. Eto, Y. Hamada, M. Kurachi, and M. Nitta, *Phys. Lett. B* **802**, 135220 (2020).
- [27] M. Eto, Y. Hamada, M. Kurachi, and M. Nitta, *J. High Energy Phys.* **07** (2020) 004.
- [28] M. Eto, Y. Hamada, and M. Nitta, *Phys. Rev. D* **102**, 105018 (2020).
- [29] M. Eto, E. Nakano, and M. Nitta, *Phys. Rev. D* **80**, 125011 (2009).
- [30] M. Eto, M. Nitta, and N. Yamamoto, *Phys. Rev. Lett.* **104**, 161601 (2010).
- [31] S. Yasui, K. Itakura, and M. Nitta, *Phys. Rev. D* **81**, 105003 (2010).
- [32] T. Fujiwara, T. Fukui, M. Nitta, and S. Yasui, *Phys. Rev. D* **84**, 076002 (2011).
- [33] C. Chatterjee, M. Cipriani, and M. Nitta, *Phys. Rev. D* **93**, 065046 (2016).
- [34] M. Kobayashi, E. Nakano, and M. Nitta, *J. High Energy Phys.* **06** (2014) 130.
- [35] Y. Hirono and M. Nitta, *Phys. Rev. Lett.* **109**, 062501 (2012).
- [36] M. G. Alford, G. Baym, K. Fukushima, T. Hatsuda, and M. Tachibana, *Phys. Rev. D* **99**, 036004 (2019).
- [37] C. Chatterjee, M. Nitta, and S. Yasui, *Phys. Rev. D* **99**, 034001 (2019).
- [38] C. Chatterjee, M. Nitta, and S. Yasui, *J. Phys. Soc. Jpn. Conf. Proc.* **26**, 024030 (2019).
- [39] A. Cherman, S. Sen, and L. G. Yaffe, *Phys. Rev. D* **100**, 034015 (2019).
- [40] Y. Hirono and Y. Tanizaki, *Phys. Rev. Lett.* **122**, 212001 (2019).
- [41] Y. Hirono and Y. Tanizaki, *J. High Energy Phys.* **07** (2019) 062.
- [42] A. Cherman, T. Jacobson, S. Sen, and L. G. Yaffe, *Phys. Rev. D* **102**, 105021 (2020).
- [43] E. Babaev, *Phys. Rev. Lett.* **89**, 067001 (2002).
- [44] Y. Tanaka, *J. Phys. Soc. Jpn.* **70**, 2844 (2001).
- [45] Y. Tanaka, *Phys. Rev. Lett.* **88**, 017002 (2001).
- [46] J. Goryo, S. Soma, and H. Matsukawa, *Europhys. Lett.* **80**, 17002 (2007).
- [47] D. T. Son and M. A. Stephanov, *Phys. Rev. A* **65**, 063621 (2002).
- [48] K. Kasamatsu, M. Tsubota, and M. Ueda, *Phys. Rev. Lett.* **93**, 250406 (2004).
- [49] M. Cipriani and M. Nitta, *Phys. Rev. Lett.* **111**, 170401 (2013).
- [50] M. Tylutki, L. P. Pitaevskii, A. Recati, and S. Stringari, *Phys. Rev. A* **93**, 043623 (2016).
- [51] M. Eto and M. Nitta, *Phys. Rev. A* **97**, 023613 (2018).
- [52] M. Eto, K. Ikeno, and M. Nitta, *Phys. Rev. Research* **2**, 033373 (2020).
- [53] M. Kobayashi, M. Eto, and M. Nitta, *Phys. Rev. Lett.* **123**, 075303 (2019).
- [54] M. Eto, Y. Hirono, and M. Nitta, *Prog. Theor. Exp. Phys.* **2014**, 033B01 (2014).
- [55] A. S. Schwarz, *Nucl. Phys.* **B208**, 141 (1982).
- [56] M. G. Alford, K. Benson, S. R. Coleman, J. March-Russell, and F. Wilczek, *Phys. Rev. Lett.* **64**, 1632 (1990); **65**, 668(E) (1990).
- [57] M. G. Alford, K. Benson, S. R. Coleman, J. March-Russell, and F. Wilczek, *Nucl. Phys.* **B349**, 414 (1991).
- [58] M. G. Alford, K.-M. Lee, J. March-Russell, and J. Preskill, *Nucl. Phys.* **B384**, 251 (1992).
- [59] J. Preskill and L. M. Krauss, *Nucl. Phys.* **B341**, 50 (1990).
- [60] M. Bucher, H.-K. Lo, and J. Preskill, *Nucl. Phys.* **B386**, 3 (1992).
- [61] H.-K. Lo and J. Preskill, *Phys. Rev. D* **48**, 4821 (1993).
- [62] S. Bolognesi, C. Chatterjee, and K. Konishi, *J. High Energy Phys.* **04** (2015) 143.
- [63] A. P. Balachandran and S. Dugal, *Int. J. Mod. Phys. A* **17**, 1149 (2002).
- [64] A. P. Balachandran and S. Dugal, *Phys. Rev. D* **66**, 034018 (2002).
- [65] M. Nitta and N. Shiiki, *Phys. Lett. B* **658**, 143 (2008).
- [66] E. Nakano, M. Nitta, and T. Matsuura, *Phys. Lett. B* **672**, 61 (2009).
- [67] M. Eto, E. Nakano, and M. Nitta, *Nucl. Phys.* **B821**, 129 (2009).
- [68] Y. Fujimoto and M. Nitta, *Phys. Rev. D* **103**, 054002 (2021).
- [69] Y. Fujimoto and M. Nitta, *Phys. Rev. D* **103**, 114003 (2021).
- [70] Y. Fujimoto and M. Nitta, *J. High Energy Phys.* **09** (2021) 192.
- [71] Y. Fujimoto, K. Fukushima, and W. Weise, *Phys. Rev. D* **101**, 094009 (2020).
- [72] Y. Fujimoto, *Nucl. Phys.* **A1005**, 121757 (2021).
- [73] I. Giannakis and H.-C. Ren, *Phys. Rev. D* **65**, 054017 (2002).
- [74] K. Iida and G. Baym, *Phys. Rev. D* **63**, 074018 (2001); **66**, 059903(E) (2002).
- [75] K. Iida and G. Baym, *Phys. Rev. D* **65**, 014022 (2001).
- [76] M. Eto, K. Kasamatsu, M. Nitta, H. Takeuchi, and M. Tsubota, *Phys. Rev. A* **83**, 063603 (2011).
- [77] K. Iida, *Phys. Rev. D* **71**, 054011 (2005).
- [78] C. Chatterjee and M. Nitta, *Phys. Rev. D* **95**, 085013 (2017).
- [79] C. Chatterjee and M. Nitta, *Phys. Rev. D* **93**, 065050 (2016).
- [80] D. F. Agterberg, *Phys. Rev. Lett.* **80**, 5184 (1998).
- [81] J. Garaud and E. Babaev, *Phys. Rev. B* **86**, 060514 (2012).
- [82] M. Nitta, *Nucl. Phys.* **B895**, 288 (2015).
- [83] M. Eto and M. Nitta, *Phys. Rev. D* **91**, 085044 (2015).
- [84] D. Gaiotto, A. Kapustin, N. Seiberg, and B. Willett, *J. High Energy Phys.* **02** (2015) 172.
- [85] Y. Hidaka, Y. Hirono, M. Nitta, Y. Tanizaki, and R. Yokokura, *Phys. Rev. D* **100**, 125016 (2019).
- [86] S. Yasui, K. Itakura, and M. Nitta, *Phys. Rev. B* **83**, 134518 (2011).
- [87] Y. Hirono, S. Yasui, K. Itakura, and M. Nitta, *Phys. Rev. B* **86**, 014508 (2012).
- [88] W. Vinci, M. Cipriani, and M. Nitta, *Phys. Rev. D* **86**, 085018 (2012).
- [89] D. T. Son and M. A. Stephanov, *Phys. Rev. D* **77**, 014021 (2008).

- [90] M. Eto, K. Hashimoto, and T. Hatsuda, *Phys. Rev. D* **88**, 081701 (2013).
- [91] C. Chatterjee and M. Nitta, *J. High Energy Phys.* 09 (2017) 046.
- [92] C. Chatterjee and M. Nitta, *Eur. Phys. J. C* **77**, 809 (2017).
- [93] C. Chatterjee and M. Nitta, *Phys. Rev. D* **101**, 085002 (2020).
- [94] M. Nitta, *J. High Energy Phys.* 03 (2021) 276.
- [95] C. Chatterjee, M. Kurachi, and M. Nitta, *Phys. Rev. D* **97**, 115010 (2018).